Captive model tests for assessing the coursekeeping of the DND Joint Support Ship contract design

Muselet, C.; Pallard, R.; National Research Council of Canada. Ocean, Coastal and River Engineering

Technical Report; no. OCRE-TR-2012-25, 2012-07-01

National Research Council Canada | Conseil national de recherches Canada

Report Documentation Page

REPORT NUMBER	PROJECT NUMBER	DATE
OCRE-~~C~~TR-2012-25	42_2517_16	July 2012

REPORT SECURITY CLASSIFICATION	DISTRIBUTION
~~Protected~~ Classification Removed October 3, 2012	~~Limited~~

TITLE
CAPTIVE MODEL TESTS FOR ASSESSING THE COURSEKEEPING OF DND JOINT SUPPORT SHIP CONTRACT DESIGN

AUTHOR(S)
C. Muselet, R. Pallard

CORPORATE AUTHOR(S)/PERFORMING AGENCY(S)
National Research Council Canada – Ocean, Coastal and River Engineering

PUBLICATION
N/A

SPONSORING AGENCY(S)
Department of National Defence, Joint Support Ship Project Management Office

RAW DATA STORAGE LOCATION(S)	PEER REVIEWED
\\NRCsjsFS1\Testdata\Test_pj2517\CWT\June_2012\pmm	No

MODEL #	PROP #	EMBARGO PERIOD
911	106R	

PROJECT	GROUP	PROGRAM
JSS-Contract Design Model Tests	Research	Performance Evaluation

FACILITY		
Towing Tank		

KEY WORDS	PAGES	FIGS.	TABLES
PMM, Manoeuvring, Directional Stability, Model 911, Joint Support Ship	i-ix, 1-31, App A-J	24	12

SUMMARY
This report describes the captive model manoeuvring tests carried out using the planar motion mechanism (PMM) on a model (Model 911) of the contract design for the Joint Support Ship for the Department of National Defence (DND). The experiments were used to assess the controls-fixed stability of the ship.

ADDRESS NRC - Oceans, Coastal and River Engineering – St. John's, Arctic Avenue, P. O. Box 12093
St. John's, NL A1B 3T5 Tel.: (709) 772-5185, Fax: (709) 772-2462

Canada

National Research Council Canada
Conseil national de recherches Canada

Ocean, Coastal and River Engineering
Génie océanique, côtier et fluvial

~~PROTECTED~~
Classification Removed

CAPTIVE MODEL TESTS FOR ASSESSING THE COURSEKEEPING OF THE DND JOINT SUPPORT SHIP CONTRACT DESIGN

OCRE-~~C~~TR-2012-25

C. Muselet, R. Pallard

July 2012

LIST OF TABLES

LIST OF FIGURES

LIST OF ABBREVIATIONS AND NOTATIONS

DND	Department of National Defence
NRCSJS	National Research Council St. John's
OCRE	Ocean, Coastal and River Engineering
IOT	NRC Institute for Ocean Technology: former name of OCRE St. John's
PMM	Planar Motion Mechanism
JSS	Joint Support Ship
SWEET	SoftWare Environment for Experimental Technologies
t	tonne(s)
m	meter(s)
s	second(s)
kts	knots
N	Newton(s)
N-m	Newton-meter
mV/V	millivolt(s) per volt
kg	kilogram(s)
deg	degree(s)
Hz	Hertz
rps	rotation(s) per second
ω	Angular frequency of harmonic motion
ω'_1	Non-dimensional angular frequency, $\omega L/U$
T	period of harmonic motion
Lpp	Length between perpendiculars
F_D	Tow force
ρ_M	Tow tank water density
S_M	Model hull surface area
V_M	Model speed
C_{FM}	Model frictional resistance coefficient – ITTC 57 model-ship correlation line
C_{FS}	Ship frictional resistance coefficient
C_A	Model-ship correlation allowance
Fr	Froude number
P	Origin of PMM balance (see Section Outfitting:)
O	Model/ship origin (see Section Model origin and coordinate system:)
(O, x*, y*, z*)	Ship-fixed coordinate system (see Section 5.1)
(O, x, y, z)	Hybrid coordinate system (see Section 5.1)
X1	PMM balance longitudinal load cell force
Y1	PMM balance aft lateral load cell force
Y2	PMM balance forward lateral load cell force
Z1	PMM balance aft port vertical load cell force
Z2	PMM balance fwd port vertical load cell force
Z3	PMM balance starboard vertical load cell force
FX	Measured surge force
FY	Measured sway force
FZ	Measured vertical force
MX	Measured roll moment at ship origin O
MY	Measured pitch moment at ship origin O

MZ	Measured yaw moment at ship origin O
MX(P)	Measured roll moment at balance origin P
MY(P)	Measured pitch moment at balance origin P
MZ(P)	Measured yaw moment at balance origin P
X	Hydrodynamic longitudinal force in hybrid coordinates
Y	Hydrodynamic lateral force in hybrid coordinates
K	Hydrodynamic roll moment at O in hybrid coordinates
N	Hydrodynamic yaw moment at O in hybrid coordinates
m	Mass of the oscillating system
G	Centre of gravity of the system
x^*_G, z^*_G	Coordinates of G in the ship-fixed coordinate system
$I_{xx}, I_{yy}, I_{zz}, I_{xz}$	Mass moments and products of inertia of the system about the ship-fixed coordinate axis (through ship origin O).
u	Surge velocity at O in the hybrid coordinate system
v	Sway velocity at O in the hybrid coordinate system
p	Roll rate in the hybrid coordinate system
r	Yaw rate in the hybrid coordinate system
φ	Roll angle in the hybrid coordinate system, in radians
ψ	Yaw angle in the hybrid coordinate system, in radians
$\dot{u}$, udot	Time derivative of u
$\dot{v}$, vdot	Time derivative of v
$\dot{r}$, rdot	Time derivative of yaw rate
$\dot{p}$, pdot	Time derivative of roll rate
ρ	Water density
L	Reference Length (=Lpp)
U	Instantaneous velocity along the trajectory: $U = \sqrt{(u^2 + v^2}$
U_{ref}	Reference velocity (approach speed of a manoeuvre)
Δu	= u-Uref
d, d'	Rudder angle, in radians
X'	Non-dimensional hydrodynamic longitudinal force
Y'	Non-dimensional hydrodynamic lateral force
K'	Non-dimensional hydrodynamic roll moment at O
N'	Non-dimensional hydrodynamic yaw moment at O
t	time
a_{kF}, b_{kF}	k-th Fourier coefficients of the quantity F (see Section 5.5)
u'	non-dimensional u
Δu'	non-dimensional Δu
v'	non-dimensional v
r'	non-dimensional r
v'_1	Non-dimensional amplitude of sway velocity (see Section 5.5)
r'_1	Non-dimensional amplitude of yaw velocity (see Section 5.5)
$\dot{v}'_1$, v'_1dot	Non-dimensional amplitude of sway velocity derivative (See Section 5.5)
$\dot{r}'_1$, r'_1dot	Non-dimensional amplitude of yaw velocity derivative (See Section 5.5)
A'	Non-dimensional constant term in the solution of motions after a disturbance from straight-line course (see Section 3.0)

B'	Non-dimensional constant term in the solution of motions after a disturbance from straight-line course (see Section 3.0)
C'	Non-dimensional constant term in the solution of motions after a disturbance from straight-line course, and stability criterion (see Section 3.0)
σ_1, sigma1	Stability index (see Section 3.0)

EXECUTIVE SUMMARY

This report describes manoeuvring experiments carried out on a 1:29.78 scale fully appended model of the Contract Design of the Joint Support Ship (JSS) in the Oceans, Coastal and River Engineering (OCRE) Towing Tank in June/July 2012. The purpose of this phase of the experiments was to evaluate performance of this revised design of the JSS in terms of its controls-fixed directional stability. Revised design featured modifications to bulbous bow and stern region to correct deficiencies observed in the Preliminary Design of the JSS.

Summary Results

This design represents an improvement on the preliminary design of the JSS in terms of controls-fixed directional stability. Yet the vessel remains unstable, with an estimated stability index σ_1 of 0.14. Besides the assessment of directional stability of the Contract Design, the experiments demonstrated that stability could be further improved by the use of a larger rudder.

CAPTIVE MODEL TESTS FOR ASSESSING THE COURSEKEEPING OF DND JOINT SUPPORT SHIP CONTRACT DESIGN

1.0 INTRODUCTION

This report describes planar motion mechanism (PMM) experiments carried out on an appended 1:29.78 scale model of the contract design for a DND Joint Support Ship (JSS), designated model911, in the National Research Council Canada St. John's (NRCSJS) Towing Tank in June and July 2012. The purpose of these experiments was to assess the controls-fixed course stability (straight-line stability) of the contract design of the JSS.

This document includes a description of the theory, of the facilities used, of the instrumentation, of the test program, of the data analysis procedure, and a discussion of the results. The PMM tests described here were carried out in the Towing Tank during two sessions: between June 11 and June 18, 2012 and between July 9 and July 12, 2012. This report is a contractual deliverable to the DND published in partial fulfillment of the NRCSJS obligations included in the Letter of Agreement between DND and the National Research Council (NRC) dated April 5, 2012.

2.0 BACKGROUND

BMT Fleet Technology (BMT) is developing the design of this vessel for the JSS Project Office. BMT is the project's Engineering, Logistics and Management Services (ELMS) contractor. The construction of up to three new vessels is planned and they are intended to replace the Navy's current Auxiliary Oiler Replenishment vessels. Further information on the JSS project can be found in Reference [1].

Free-running manoeuvring model tests conducted on the pond in the fall of 2011 on a model of the preliminary design of the JSS, highlighted problems with the directional stability of the ship. This raised a concern, as one of the missions of the ship is replenishment at sea. PMM tests were conducted on the preliminary design in January 2012 to determine the stability index: they confirmed that the ship lacked straight-line stability; they also showed that it was possible to improve the stability by adding appendages, albeit with a powering penalty.
Consequently the bulb and stern of the vessel were re-designed, and the resulting contract design of the JSS is being assessed in this phase, by means of captive model tests with the PMM to determine the straight-line stability index.

3.0 THEORY

Controls-fixed stability characterizes the response of the ship to an external force or moment disturbing the ship from its initial straight-line path. Controls-fixed stability is an important element of path keeping at sea, along with other elements of the control loop such as the characteristics of response of the steering gear to a deviation from the path. In

the case of a surface ship, the only controls-fixed stability possible is straight-line stability: after a disturbance, the ship would return to a straight-line path, albeit in a different direction. Such dynamic course stability is desirable, as a lack of it would put strain on the steering and autopilot systems.

To analyze the problem of course stability, Newton's equations of motion are written. In the absence of wind, waves, current and other external forces such as from a tug, the external forces and moments that act on the ship are the hydrodynamic forces acting on the hull and appendages. The equations are written in ship-fixed axis, with origin at the centre of gravity of the ship.

The surge and sway force components X and Y and yaw moment component N of the hydrodynamic forces are functions of the velocities and accelerations of the ship: $X, Y, N = f(u, v, \dot{u}, \dot{v}, r, \dot{r})$.
These functions are reduced to a simple mathematical model through the use of Taylor expansion, developing the functions near the values of the variables at the initial equilibrium position. Considerations of symmetry about the xz plane for ships in general (although not quite exact for a single propeller ship) permit simplification of these functions. Details can be found in Reference [2]. Further, since the study of motion stability considers very small changes in variables from the initial equilibrium position, the equations are linearized.

The linearized equations of motion are, in moving axis with the origin at the centre of gravity:

$$\begin{aligned} -X_u(u-u_1) + (m-X_{\dot{u}})\dot{u} &= 0 \\ -Y_v v + (m-Y_{\dot{v}})\dot{v} - (Y_r - mu_1)r - Y_{\dot{r}}\dot{r} &= 0 \\ -N_v v - N_{\dot{v}}\dot{v} - N_r r + (I_z - N_{\dot{r}})\dot{r} &= 0 \end{aligned} \tag{1}$$

In non-dimensional form (see details of non-dimensionalization in Section 5.2), considering only the sway and yaw moment equations of interest in the study of course stability, and considering that for usual ship configurations $Y'_{\dot{r}} \approx 0$ and $N'_{\dot{v}} \approx 0$, two simultaneous first order differential equations are obtained:

$$\begin{aligned} (m' - Y'_{\dot{v}})\dot{v}' - Y'_v v' - (Y'_r - m')r' &= 0 \\ (I'_z - N'_{\dot{r}})\dot{r}' - N'_v v' - N'_r r' &= 0 \end{aligned} \tag{2}$$

where the hydrodynamic derivatives are those evaluated with the rudder fitted and at rudder angle $\delta_R = 0$.

The solutions are of the form:

$$\begin{aligned} v' &= V_1 e^{\sigma_1 t} + V_2 e^{\sigma_2 t} \\ r' &= R_1 e^{\sigma_1 t} + R_2 e^{\sigma_2 t} \end{aligned} \tag{3}$$

With:

$$\sigma_1 = \frac{1}{2}\left(-\frac{B'}{A'} + \left[\left(\frac{B'}{A'}\right)^2 - 4\frac{C'}{A'} \right]^{\frac{1}{2}} \right)$$
$$\sigma_2 = \frac{1}{2}\left(-\frac{B'}{A'} - \left[\left(\frac{B'}{A'}\right)^2 - 4\frac{C'}{A'} \right]^{\frac{1}{2}} \right) \quad (4)$$

where:

$$A' = (I'_z - N'_{\dot{r}})(m' - Y'_{\dot{v}})$$
$$B' = -(I'_z - N'_{\dot{r}})Y'_v - (m' - Y'_{\dot{v}})N'_r \quad (5)$$
$$C' = Y'_v N'_r - (Y'_r - m')N'_v$$

For the path of the ship to resume a straight-line direction, v' and r' must approach zero with time, and so both σ_1 and σ_2 must be negative. σ_1 being the largest, it constitutes a single quantitative measure of stability: for controls-fixed stability, the stability index σ_1 must be negative:

$$\sigma_1 < 0 \quad (6)$$

A study of the signs and magnitudes of quantities involved in the calculation of σ_1, considering the physics of the flow and the resulting signs and magnitudes of the hydrodynamic derivatives, permits to establish a simplified criterion for controls-fixed stability:

$$C' > 0 \quad (7)$$

The linear hydrodynamic derivatives $Y'_v, N'_r, Y'_r, N'_v, Y'_{\dot{v}}, N'_{\dot{r}}$ were evaluated by means of captive model tests carried out on the PMM. With that information in hand and knowing the mass properties for the ship, the sign of C was determined and the stability index σ_1 was evaluated.

The model was ballasted to the proper scaled ship draft and trim, and was propelled at the ship self-propulsion. The longitudinal centre of gravity and yaw radius of gyration did not need to be scaled to those of the ship: the model mass properties were measured and the model inertial forces were subtracted from the balance measurements to obtain the hydrodynamic forces and hydrodynamic coefficients.

4.0 EXPERIMENTS

4.1 Description of the NRCSJS Towing Tank

The NRCSJS Towing Tank has dimensions of 200 m by 12 m by 7 m with a dual-flap wavemaker fitted at one end. A wave absorber consisting of a parabolic beach is fitted at

the opposite end. Flexible side absorbers can also be deployed along the entire length of the tank to minimize the time between runs. The 80 tonne tow carriage capable of speeds up to 10 m/s is used to accommodate models for a wide range of test types carried out in calm water or waves. Additional information on the Towing Tank is provided in Reference [3].

4.2 NRCSJS Planar Motion Mechanism

The NRCSJS new PMM was designed and fabricated by Cussons Technology Ltd. of Manchester, U.K. to be installed under the main carriage in either the Ice Tank or the Towing Tank, and is used in ship manoeuvring studies conducted in ice and open water. The motion of the sway and yaw axis is controlled by the PMM motion control drive system conforming to a user defined vector profile while hydrodynamic or ice induced forces and moments are recorded on a dedicated integral 6-component dynamometer. The drive system also outputs a surge demand signal controlling the forward speed of the main carriage. The model can be held fully captive however generally for open water experiments the model is free to pitch and heave. In cases where the roll motion is deemed to have a significant influence on the manoeuvring performance (for example if the ship has a low metacentric height) the roll angle can be manually adjusted to ±30 degrees.

In open water, hydrodynamic coefficients derived from PMM experiments carried out with a physical model fitted are used to simulate standard ship manoeuvres by providing a solution of the Abkowitz mathematical model (described in Reference [4]). Standard experiments include stationary straight-line tests (straight or oblique towing with/without rudder deflection) as well as harmonic tests (pure sway, pure yaw, pure yaw with drift, combined sway and yaw). Typical manoeuvres capable of being predicted include turning circles, zigzags, spirals, Williamson (man overboard) Turn etc.

A system schematic of the PMM is provided in Figure 1. A general description and operating manual for the PMM is available in Reference [5].

4.3 Description of Physical Model 911

Fabrication:

Model 911 is a 1:29.779 scale, nominally 6 m long, representation of the contract design of the Joint Support Ship fabricated using a polystyrene foam core with ¾" plywood and Renshape™ for areas requiring reinforcement as described in the NRCSJS model fabrication standard provided in Reference [6]. The foam was milled to conform to the desired hull geometry using the NRCSJS Liné milling machine. The model was complete up to the deck at 15.25 m full scale: this height corresponds to the Replenishment at Sea (RAS) deck. The model was then painted with three coats of polyurethane yellow. Standard markings were included on the model as described in NRCSJS model construction standard (Reference [6]). Renshape™ inserts were included in the hull to add reinforcement in way of the hull penetrations and in way of the location

of the bilge keels. A lateral bow tunnel thruster was included in the model. A rudder post and stern tube were embedded in the hull. A total of 14 milled surfaces capable of accommodating trim hooks were included along the main deck to provide flexibility when verifying the model attitude in the tank. Attachment locations for the model steel frame that interfaces with the PMM balance, were surveyed and marked during milling to provide references for mounting the PMM force balance aligned precisely with the centreline of the model.

The body plan, profile drawing and plan view are provided in Figures 2 and 3.

Outfitting:

Cylindrical stud turbulence stimulators were fitted to the bow and bulb as per NRCSJS Standard (Reference [6]) and shown in Figure 4. The bow thruster tunnel was fitted on centreline with an acrylic plate cut to represent approximately the side area of a four-bladed propeller, as illustrated in Figure 5.

A removable rudder was fabricated that conformed to the ship rudder design (referred to as “design rudder”). Bilge keels were fitted to the hull. Two larger centreline rudders were also tested, that had been designed by NRCSJS for the January 2012 session. They are referred to as “Rudder 2” and “Rudder 3”, and are illustrated along with the design rudder in Figure 6. The dimensions of all rudders are given in Table 1.

A pull point, consisting of an eye bolt fixed to the transom on the longitudinal centerline, was designed to enable daily longitudinal pulls nominally 3 cm above the base of the transom to check consistency of the longitudinal force load cell. Lifting lugs were included on the model providing attachment points for the bifilar suspension used to verify the yaw gyradius of the model.

The PMM force balance interface steel frame was mounted to the plywood bottom in the forward cockpit of the model then the PMM balance was attached onto the frame. Once it is mounted to the PMM tow post, the model is permitted freedom to pitch and heave about the balance pivot point located 1.9 cm forward of amidships, 5.2 cm below the design waterline, and on the model longitudinal centreline. The location of the PMM balance in the model is illustrated in Figure 7.

The model was fitted with the five-bladed stock propeller P106R, right-turning, of diameter 191.41mm and fixed pitch 186.29mm.

The model shaft was fitted with an Aerotech propulsion motor, enveloped by a light metal mesh screen to isolate the instrumentation from RF noise, and controlled by a Soloist CP single-axis digital servo controller. The rudder was controlled using an SSPS-105 precision electro-mechanical servo.

The shaft motor, rudder servo and onboard data acquisition system can be seen mounted in the model in Figure 8. Figure 9 shows the bow of the model as connected to the PMM.

Model particulars:

The model was tested fully appended with bilge keels and rudder fitted, in the following displacement condition: nominally 23948 m^3 volume of displacement, level trim at 8.2 m draft full scale.

The length between perpendiculars (Lpp) of the ship is 174.846 m (5.871 m at model scale).

The hydrostatics for the ship and model for the test condition can be found in Tables 2 and 3.

Model origin and coordinate system:

We define a ship/model origin O, around which manoeuvring motions are defined and moments and hydrodynamic coefficients are calculated. For this vessel the origin was chosen to be on the centreline, amidships, at the 8.2 m draft design waterline.

A model coordinate system is defined, that has its origin at O, its longitudinal axis along the centreline of the model pointing forward, its vertical axis in the symmetry plane of the model pointing down, and its transverse axis pointing to starboard.

The ship/model origin and coordinate system are illustrated in Figure 10.

Because the centre of gravity of the ship does not coincide with the origin O where hydrodynamic coefficients are evaluated, additional terms appear in the expressions for A', B', C', that were not shown in equations 5. However, the ship centre of gravity is only 0.5m forward of the origin and it was verified that these additional terms are negligible in the calculation of C' and σ_1.

Mass properties:

The model is captive during the tests therefore mass properties need not match full-scale properties. However, the actual mass properties of the oscillating system as seen by the balance during model tests must be known in order to subtract inertial forces and moments from the measured forces and moments. This oscillating system consists of the ballasted and outfitted model, together with the live part of the force balance. It excludes the ground part of the force balance and the tow post (see Section 5.1).

The mass properties of the live and ground parts of the balance are known from the manufacturer documentation and from earlier determination.

In order to determine the vertical centre of gravity, prior to connecting the model to the PMM an inclining experiment was conducted on the fully ballasted model fitted with the

PMM balance and a dummy tow post. The moment of mass of the dummy tow post and moment of mass of the ground part of the balance were subtracted numerically.

The longitudinal centre of gravity and the mass moment of inertia about the vertical axis of the model coordinate system (through model origin O) were determined after the manoeuvring tests were completed, using a bifilar torsion pendulum experiment, with the model fully outfit and ballasted in its test condition but without the PMM balance. The moment of mass and the moment of inertia of the live part of the balance were added numerically.

The mass properties of the oscillating system are summarized in Table 4.

4.4 Description of Instrumentation and Data Acquisition System

Instrumentation and calibration:

A list of signals measured is given in Table 5.
Calibration information for all signals is provided in Appendix A: Instrumentation Calibration Information.

Carriage Speed:
Carriage speed is calibrated periodically by setting up two proximity switches on the Tow Tank rails at a measured distance apart with companion switches on the tow carriage linked by cable to the carriage data acquisition system. The tow carriage is operated at a constant speed between the two switches and the time between activating the switches recorded on the carriage data acquisition system - thus providing an accurate measure of tow carriage speed.

Two separate carriage speed measurements are available: one from the carriage control system, obtained by processing pulse count information from a touch roller; and another from a tachogenerator connected to one of the eight drive shafts. Here the tachogenerator measurements were used in all analysis.

The carriage speed was calibrated over a range from 0.5 to +2 m/s.

Six component force/moment balance:
A six (6)-component force/moment balance provided by Cussons as part of the PMM outfit is ideally mounted in the model such that the origin P of the balance, defined as the point around which the model is free to pitch, is located as close to the origin of the model as feasible. In this case, the location of the origin P of the balance relative to the model origin O was 0.019 m forward and 0.052 m below.

The PMM balance was fitted with the following load cells for these experiments:
Longitudinal force load cell X1= 500 N
Two lateral force load cells Y1, Y2 = 1920 N
Three vertical force load cells Z1, Z2, Z3 = 1920 N

The rating of the balance (not combined) for forces and moments at the balance origin P was thus:
Drag Force FX = ± 500 N
Sway Force FY = ± 3840 N
Heave Force FZ = ± 4800 N
Yaw Moment MZ(P) = ± 1920 N-m
Pitch Moment MY(P) = ± 1,690 N-m
Roll Moment MX(P) = ± 480 N-m

The larger of two sets of lateral load cells available for the PMM balance were fitted for these tests.

The PMM balance was calibrated using a dedicated calibration stand supplied by Cussons with the PMM, and using a procedure where only one force or one moment is applied to the balance at any one time, as described in Reference [5]. A calibration had been carried out just prior to the January 2012 test session, albeit with smaller lateral force load cells Y1 and Y2. The calibration data was analyzed to yield a "global" calibration matrix, which transforms individual load cell outputs in mV/V into forces and moments at balance centre P in engineering units. Given that the PMM balance load cells are sensed and the calibration matrix is applied to load cell outputs in mV/V, the calibration matrix is independent from the acquisition system. Actual excitation voltages at any given time must be known: they were recorded during calibration and then on each day of the test session, although they did not vary significantly over the course of the test session.

From this "global" calibration matrix and using a nominal geometry matrix for the balance (the geometry matrix reflects the relative location of the load cells), a "cross-talk" matrix was derived that isolates the cross-talks between load cells in the PMM balance. The cross-talk matrix is presented in Appendix B: PMM Balance: Calibration Matrix and Calculation of Forces and Moments. It can be seen that the cross-talks are very small: the terms in the "global" calibration matrix reflect mostly the load cell sensitivities and the balance geometry.

To calculate forces and moments, the mV outputs of the balance load cells were divided by their excitation voltage, and multiplied by the load cell sensitivity to obtain forces in Newtons. Then the crosstalk matrix was applied, and the geometry matrix to obtain forces and moments at the balance centre P. Lastly, those forces and moments were transferred to the model origin O. The load cell sensitivities and the geometry matrix are provided in Appendix B: PMM Balance: Calibration Matrix and Calculation of Forces and Moments..

Note that heave force FZ and pitch moment MY are not meaningful for a model free to pitch and heave.

Sinkage and Pitch Angle:
Pitch angle was measured using the rotary transducer supplied by Cussons integral with the PMM balance. It was calibrated against a digital inclinometer, over a range of ±4 degrees. As per the standard OCRE sign convention described in Reference [7], pitch angle is positive bow up.

Sinkage was measured with a yo-yo potentiometer mounted on the tow post. Sinkage is therefore measured and given at a point 0.022 m forward of midships. The sinkage displacement sensor was calibrated using a dedicated apparatus whereby the yo-yo potentiometer cable was attached to a flat plate such that the cable could be adjusted in discrete increments a known distance from the sensor. As per the standard OCRE sign convention described in Reference [7], sinkage is positive down.

PMM Sway Velocity & Yaw Rate:
PMM Sway velocity in tank axis and PMM yaw rate were measured using Cussons supplied instrumentation incorporated into the PMM. Factory calibration factors were used. The sway velocity had a calibrated measuring range of ±1 m/s while the yaw rate had a calibrated measuring range of ±27 degrees/second.

PMM DAS Trigger:
PMM DAS Trigger is a step signal sent from the PMM control system, used to identify the exact start time of an input PMM motion. It was split and passed through two channels of an Isolation Amp and fed to both the Carriage Data Acquisition System and the in-model Data Acquisition System, DasPC49 (see "Data Acquisition System further in this Section).

PMM Sway Displacement and Yaw Angle:
Sway displacement of the PMM in tank axis was measured with a yo-yo potentiometer with a 500 inch (1270 cm) range attached to the PMM frame. To calibrate this sensor prior to mounting it, the end was attached in a fixed point behind the carriage, the carriage was moved forward and the sensor output was compared to carriage position as output by the carriage instrumentation.

PMM Yaw Angle was measured using a yo-yo potentiometer with a 75 inch (190.5 cm) range wound around a strap fixed to a rotating segment of the PMM and anchored to a static point on the PMM frame. The methodology used to calibrate this sensor was to rotate the PMM through a series of yaw angles (±30 degrees) with the tow carriage stationary and compare the output from the potentiometer to the commanded yaw angle.

Sway displacement and yaw angle measurements were reset to zero every morning with the PMM commanded to zero sway displacement and yaw angle. Note that these two NRC-added measurements are not used in driving the PMM: the PMM motion control drive system takes feedback from its own internal sensors, although no output is available from these sensors. Neither is the sway displacement or the yaw angle measurement used in any of the analysis: for analysing static tests and deriving hydrodynamic coefficients,

yaw angle is taken to be its nominal value, as input to the PMM. In the processing of dynamic runs, yaw angle is calculated by integrating yaw velocity, a PMM sensor.

Rudder Angle:
The rudder was powered by a SSPS-105 precision electro-mechanical servo and controlled via OCRE Remote Control Software. Rudder angle was measured at the rudder shaft using a Vishay Spectrol Model 132 single turn precision potentiometer. This device was mounted to the aft coaming and attached to the rudder shaft with a flexible coupling. Both the servo and the potentiometer were calibrated against a protractor quadrant fitted in the model adjacent to the linkage and the calibration was stored in the remote control software. A third order calibration was used for the potentiometer, over a range of ±35 degrees. In this experiment, rudder angle was set to discrete rudder angles. As per the standard OCRE sign convention described in Reference [7], positive rudder angle is with trailing edge to port side.
Any time that the rudder was fitted to the hull, its trailing edge was aligned visually along the marked centreline, and the Rudder Angle channel was re-zeroed for that position.

Propeller shaft speed:
Shaft speed was measured using an Allegro A3422 Hall-Effect, Direction-Detection Sensor combined with a Maxim 525 digital-to-analog converter. The calibration was verified using a hand-held digital tachometer. The calibrated measuring range was 4 to 20 rotations per second (rps).

Thrust and Torque:
Shaft thrust and torque were measured with a Kempf and Remmers dynamometer (K&R R-250) dynamometer calibrated using a dedicated apparatus as described in Reference [8]. The shaft torque sensor was calibrated through a range of ±5 N-m while the shaft thrust sensor was calibrated through a range of 0 to 150 N.

Water Temperature:
Water temperature was periodically measured manually by dragging a hand-held digital thermometer below the water surface at about the nominal draft depth.

Data Acquisition System:

With the exception of the two signals for the PMM motion trigger, all data was acquired at 50Hz and low pass filtered at 10 Hz, amplified as required. The PMM trigger signal is a step signal output by the PMM that indicates the exact start of the PMM motion, and it was acquired on both acquisition systems for verifying synchronization. It was acquired at 500Hz and filtered at 100Hz.

All signals were transferred to the data acquisition systems via cable, conditioned/ digitized using two separate systems: a PC-based acquisition system (DasPC49) located inside the model for most channels, with the exception of both carriage speed channels, PMM sway velocity and PMM yaw rate, PMM sway displacement and the inline load cell which were acquired on the carriage NEFF acquisition system (TowDas). The PMM

Sway velocity and PMM yaw rate signals were isolated from the TowDas through an 8-Channel Isolation Amp. This configuration was chosen in an effort to minimize noise on the measurements induced by the PMM motors. The in-model acquisition system was powered by batteries located in the model.

The model-based data acquisition system used for this test consisted of two "8-channel high speed signal conditioners" (HSC8). These HSC8 units include input radio frequency rejection, low temperature drift amplification, selectable filtering, a very stable sensor excitation reference and output signal offset adjustment. The inputs can accommodate current, voltage and resistive signals. These HSC8's were designed, developed and fabricated at NRCSJS. The high-speed signal conditioner was designed for field or trials impact measurements. Data from this system has been observed to have a low base noise performance similar to, or exceeding, that of the carriage-based NEFF systems. The other components in the acquisition system for this model consisted of a National Instruments 32-channel NI USB-6218 and a computer running the NRCSJS standard data acquisition system and software as described in Reference [9]. General description of the carriage based NEFF data acquisition system is also furnished in Reference [9].

4.5 Description of the Experimental Setup

Towing Tank and PMM Setup

Water Depth:
The water depth is fixed at nominally 7 m.

Side Beaches:
Flexible side beaches were deployed over the entire length of the tank to absorb the lateral waves and minimize the time between runs. The requested wait time between runs was 12 minutes.

Run Length:
Test runs were carried out with the carriage running towards the wave-maker. The PMM control system was used to control the tow carriage for most runs. The available run length for experiments was from tow tank position 20.5 m to tow tank position 158.5 m.

Alignment of PMM:
When the new IOT PMM was commissioned and installed for the first time onto the tow carriage, it was ensured using laser technology that the PMM was aligned along the centreline of the tank when PMM Yaw angle was set at zero. Positioning references and attachment points for the PMM onto the carriage frame were machined while the PMM was in that surveyed position. Furthermore, the PMM Yaw zero position is indicated by a hardware switch and is thus replicable.

Pull Point:
The pull point apparatus used to carry out daily verification of the PMM longitudinal force load cell was installed on the carriage longitudinal centreline at the outboard edge at the east end of the tow carriage to enable a standard series of weights to be applied at the beginning of every test day. The load applied to the stern was measured using a waterproof inline load cell.

Model setup

The model was launched and was ballasted to its target displacement and trim hook settings. An inclining experiment was conducted to determine the vertical centre of gravity.

The model was connected to the PMM tow post, free to heave and pitch. A short set of check and procedural tests were conducted without propeller, with friction hub, and then the propeller was installed. A final check of the trim hook settings was done at that stage.

4.6 Description of the Test Program

The test log is presented in APPENDIX C: Test Log.

The contract design for the JSS was assessed in a first test session between June 11th and June 19th, 2012. The first session also included a full test matrix for a determination of third order hydrodynamic coefficients, but the full test matrix is not addressed in this report: only the sub-matrix for determination of the controls-fixed linear coefficients. In a second session between July 9th and July 12th, 2012, the controls-fixed test matrix was repeated on the same model configuration, in order to assess repeatability and evaluate the order of magnitude of uncertainty in the determination of hydrodynamic coefficients due to experimental setup. Then in that second session the test matrix was repeated with two larger centreline rudders, labelled Rudder 2 and Rudder 3 (illustrated in Figure 6)

Test Matrix

The controls-fixed manoeuvring test matrix is presented in Table 6.

All tests were conducted for an approach speed of 18 knots full scale (1.697 m/s model scale), speed of interest specified in the Statement of Work. The Froude number at 18 knots is 0.22.

The test matrix comprised three types of tests to provide the required hydrodynamic coefficients:

- "Static" drift tests, to extract the coefficients relative to model sway velocity v.
- Pure harmonic sway tests, to extract the coefficients relative to sway rate $\dot{v}$. Coefficients in v can also be extracted from these tests, and they can be compared to the results of the drift tests.

- Pure harmonic yaw tests, to extract the coefficients relative to yaw rate r and those relative to yaw acceleration $\dot{r}$.

During the drift tests, a sweep through rudder angles -10 deg and +10 deg was also done although not needed for the controls-fixed study, because three rudder angles could be fitted in one run length.

The OCRE software and the method used for extracting hydrodynamic coefficients from PMM tests consider the nonlinear equations of motion with a third order mathematical model of hydrodynamic forces and moments. This method yields both the linear and nonlinear hydrodynamic coefficients. Consistently with this method, the range of test parameters was chosen to include the full range of kinematic values expected during manoeuvres of the vessel, and not just the linear range: drift angles up to 20 degrees were tested, and non-dimensional yaw rates up to 0.6 (non-dimensional yaw rate: $r' = r\frac{L}{U}$; see Section 5.2). The larger range of motion amplitudes was preferred, as force measurements from very small amplitude motions carry relatively more noise.

The model was propelled at the nominal ship self-propulsion point, determined for the straight-line speed of 18 knots. The self-propulsion shaft speed was obtained from self-propulsion runs that had been carried out on model 911 prior to the PMM tests. Based on these prior tests, a model shaft speed command of 9.96 rps was chosen, yielding the amount of towing force corresponding to ship self-propulsion as per Section 4.6 of Reference [10]:

$$F_D = \frac{1}{2}\rho_M S_M V_M{}^2 * (C_{FM} - (C_{FS} + C_A)) \text{ with } C_A = 0.0002$$

The oscillation frequency of harmonic runs was carefully selected in consideration of the ITTC recommendations and guidelines (see Reference [11]). The chosen harmonic period must be long enough to avoid both tank resonance and non-stationary lift and memory effects. On the other hand, if the period is too long the number of cycles that fit in the length of the tank will be insufficient, and the lateral amplitude of motions required for achieving the highest of the required yaw rates will cause hydrodynamic interference of the model with the tank walls. The maximum non-dimensional frequency $\omega_1' = \omega L/U$ that is recommended for avoidance of non-stationary effects is 1-2 for sway, and 2-3 for yaw tests. For each type of harmonic test (sway or yaw), one appropriate value of frequency was selected below the recommended maximum. This frequency was also chosen such as to keep the model within the half-width of the tank or close, while permitting a minimum of four cycles in the length of the tank. In each set of pure harmonic runs, sway or yaw, one run at an additional frequency was also included to verify that frequency had been chosen low enough to have little influence on the results.

The definitions and characteristics of all motions to be executed by the PMM for this model are presented in Table 7 (static tests) and Table 8 (harmonic tests).

The vector profiles for typical PMM runs are illustrated in Figure 11.

A number of repeat runs were included in the test matrix to verify repeatability.

It must be noted that due to concerns regarding oscillating the 80+ tonne mass of the tow carriage with PMM fitted, compounded with the fact that the control of carriage speed by the PMM is poorly synchronized with the lateral and angular motion signals, carriage speed variation by the PMM control system is not currently enabled, other than for acceleration and deceleration to target speed. Carriage speed during a run was therefore always constant. The consequence is that the "pure" harmonic yaw motions contain a small component of parasitic sway and surge rates in model coordinates.

Quality Control Tests

Initially, the shaft bearings were run in as described in the IOT standard for self-propulsion experiments (Reference [12]). No water leakage through the stern tubes was noted.

Shaft Friction Torque (as per Section 4.2.6 of Reference [12]): Values were determined with the model stationary for eight values of shaft speed from 3.8 to 11.0 rps. Determination of the shaft friction torque was not deemed critical to meet the goals of the manoeuvring program, and the shaft friction was simply monitored. Mean value statistics were computed for each of the steady state shaft speed data segments. Shaft torque was plotted versus shaft speed and is shown in Figure 12.

Model Alignment Check: To assess the alignment of the model relative to the tank longitudinal axis, at the start of the test program runs were carried out at drift angles -5, 0 and +5 deg, at 1.697 m/s, with the propeller turning slowly and the rudder on centreline. The data is presented in Figure 13, and the resulting yaw angles of zero lift and zero yaw moment, respectively -0.15 deg and -0.09 deg, were deemed satisfactory model alignment. The OCRE PMM does not offer a mechanism to offset the unit in yaw and remove any residual small misalignment. No attempt was made to correct yaw angle values reported and used in analysis: yaw angle was taken to be the nominal yaw angle input to the PMM.

Neutral rudder angle determination: By doing straight runs down the tank at 1.697 m/s while sweeping the rudder through small angles (±2 deg), with the propeller turning at ship self-propulsion shaft speed, the rudder angle that adds no yaw moment to the vessel was determined. This neutral rudder angle was determined to be about -1.5 deg (±0.5 deg). Harmonic runs in the test matrix were carried out at the determined "neutral" rudder angle, while static drift runs were carried out with the rudder along the centreline (and also at -10 and + 10 deg).

In-situ Propeller Check Tests: Although the propulsion data per se is not required as an input for the manoeuvring prediction model used by IOT, an accurate thrust force from the propeller imparted on the model and the PMM balance is important. Thus the propulsion parameters are monitored daily throughout the test program to ensure that the shaft is not binding or otherwise providing an erroneous influence on the vessel. In-situ checks were carried out at the beginning of each test day as described in Section 4.2.7 of Reference [12]. The model with propeller fitted was moved to the nominal longitudinal center of the Tow Tank, and the shaft speed was increased in seven steps from 1.6 to 10.0 rps. Mean value statistics were computed for shaft speed, shaft torque, shaft thrust and surge force, for each of the steady state segments. The quality of the propulsion data was evaluated by plotting the mean values of shaft thrust and torque (without a correction for shaft friction) vs. shaft speed squared. An example plot is furnished in Figure 14. The linear fit to the data is good and the value of shaft torque extrapolated to zero shaft speed equals approximately the friction torque. A plot of tow force vs. total shaft thrust was also generated. An example plot is provided in Figure 14. The linear fit to the data is good. The slopes and intercepts of the linear fit to the data for all in-situ tests are summarized in Figure 15, showing the consistency of the propulsion data through the test program.

PMM Balance Check, Longitudinal Pulls: At the start of each day, a static in-situ pull was carried out on the PMM balance to verify the PMM longitudinal force (FX) load cell, applying a load from 0 to 30 kg. The longitudinal pull data was analyzed by assessing the mean value of the applied force measured by the inline load cell and plotting against it the mean value of the calibrated longitudinal force on the PMM balance as measured by the surge force load cell. The relationship shall be linear, and the slope shall be close to 1.000 and not vary significantly from day to day. Figure 16 presents a typical pull test result plot, and a summary of linear fit parameters, slope and R-square, for all longitudinal pull tests.

PMM Balance Check, Yaw Sweeps: In order to verify consistency of the side force readings, yaw drift tests from 0 to 20 degrees in steps of 10 degrees to both port and starboard were carried out each day, at a constant forward speed of 1.697 m/s with the propeller turning at a shaft speed determined to provide approximately zero thrust. The PMM balance forces and moments from each constant drift segment of the yaw sweep runs were computed. The mean values of the longitudinal force (FX), lateral force (FY), yaw moment (MZ) and roll moment (MX) were compiled and plotted against yaw angle, and a polynomial fit was done. The results were reviewed to determine whether there was any significant variation from day to day. See Figure 17 for a typical yaw drift test result plot and a summary of the regression factors for all yaw sweep tests of the test program.

Force/Moment Repeatability Evaluation: An effort was made to check the repeatability of the data acquired. A set of selected runs were repeated. Tabular results of data repeatability for these runs are listed in APPENDIX J: Comparison of Repeat Runs. Also, the full test matrix was repeated in a second session for the JSS contract design, in July. Comparison of the resulting hydrodynamic coefficients and stability criterion and index

from both sets (see Section 6.0) is indicative of the order of magnitude of uncertainty due to experimental setup.

Typical Run Sequence

A typical resistance run sequence is provided as follows:

1. Data acquisition is commenced for 60 seconds prior to the beginning of the test run to acquire a calm water tare segment with the shafts turning slowly;
2. The shaft speed and rudder angle are set to the required value with the tow carriage still at rest;
3. Shortly afterwards, the tow carriage accelerates to the required test speed using a control signal from the PMM for all runs other than the rudder sweep where the carriage operator assumed control (and a longer run length can be used);
4. A remote screen in the carriage control room was used to conveniently set user defined discrete shaft speed and rudder angle points. The carriage operator can change the rudder angle at time intervals as the carriage progresses down the tank – the number of rudder angles per run depends on the available run length-.
5. Data acquisition continues until the termination of the run and the carriage speed decelerates to zero;
6. The carriage then returns to the starting position at a return speed of 0.5 m/s. A wait time of approximately 12 minutes between runs starting at the onset of acquisition is observed to permit the tank to settle.

4.7 Online Data Analysis

Preliminary Data Review

The data were acquired in GDAC format (*.DAQ files) described in Reference [14]. An analysis of the preliminary data was carried out on the Tow Tank carriage workstation throughout the test program to verify the data integrity. The time series data for each user-selected time segment as well as the basic statistics (minimum, maximum, mean and standard deviation) were viewed at the end of each run using the SWEET software described in Reference [15] and stored in the online test directory as a Portable Document Format (***.PDF) file. The general SWEET online data analysis routine was customized to include the conversion of the PMM balance outputs (in mV) into calibrated forces (in N) and moments (in N-m) at model origin, per the procedure described in APPENDIX A: PMM Balance: Calibration Matrix and Calculation of Forces and Moments. Two examples of a SWEET output files are provided in APPENDIX D: Example SWEET Output Files (for a static run with drift, and for a harmonic yaw run).

Pre-Processing of Manoeuvring Runs

The aim of the pre-processing is to extract either mean values (for static tests), or time series of the force and motion measurements and their decomposition in Fourier series

(for harmonic runs): these are utilized in further analysis to derive manoeuvring coefficients.

All manoeuvring runs were processed using custom routines in the SWEET software:

- One task performed by the SWEET custom routines is applying calibration data to the load cell outputs to obtain forces and moments at the balance origin P, transferring them to the model origin O, and removing from the longitudinal force the balance weight component induced as the model changes trim angle at speed.
- The time series for carriage speed, shaft speed, rudder angle, PMM sway velocity, yaw angle, side load cell forces Y1 and Y2, and PMM start, were plotted on the screen.
- Start and end times (T1, T2) were interactively selected for the initial tare segment with the model at rest and before rotating the propeller shafts, and for each segment of interest at speed.

For further specifics of the pre-processing, we distinguish between two types of tests: "static tests" where model velocities and parameters are held constant and forces and moments reach a steady state value; and dynamic tests such as harmonic runs where velocities follow a periodic time function.

For "static" tests:

1. Each steady-state segment was selected, taking care of excluding initial transient data, and aiming to select a measuring length of two to three times the model length.
2. The mean values of variables over each analysis segment after taring were written to a CSV file. The following channels were excluded from taring: carriage speed, shaft speed, shaft torque, PMM pitch and yaw angles, rudder angle.
3. Further analysis of static runs will be carried out using Excel and the CSV file containing mean values for all runs.

For harmonic runs:

1. All signals were re-sampled at 100 Hz to match the rate of the PMM drive signals.
2. A single analysis segment at speed was selected, starting precisely at the start of the PMM motion and ending anytime after carriage deceleration. The "DAS Trigger" signal was used to determine the exact start time of the analysis segment. The trailing edge of the square signal corresponds to the start of the PMM motion, but since the edge is not sharp, the leading edge time was determined and carriage acceleration time as recorded in the PMM motion file for the run was added to this time.
3. The time series of tared data for the selected analysis segment was exported to a CSV file. The following channels were excluded from taring: carriage speed channels, shaft speed and torque, PMM pitch and yaw angles, rudder angle.
4. A Python routine was then run to generate from the CSV file an input file (named "mess*xxxx*.dat" where *xxxx* is the run number) in a format suitable to the harmonic

run analysis program. The input file "mess*xxxx*.dat" contains the time records of the forces and moments at model origin O, and the time records of the measured PMM velocities at the PMM balance centre P in tank coordinates: carriage speed, PMM sway velocity and PMM yaw velocity.

5. Fourier analysis was performed by using either the analysis module "pmmana" of the software provided by HSVA for operation of the OCRE PMM or equivalent custom calculations in Excel (both yielded identical results). The measured forces and moments in non-dimensional form were thus decomposed into third order truncated Fourier series: $F = \frac{a_{0F}}{2} + \sum_{k=1}^{3} a_{kF} \cos k\omega t + b_{kF} \sin k\omega t$; where F is a general notation for either of the forces or moments; and where $a_{kF}, k = 1,3$ and $b_{kF}, k = 1,3$ are the Fourier coefficients for F(t).
6. For example, using "pmmana": in a GUI, the motion corresponding to the run was selected, and the following parameters were entered: the location of the ship origin relative to the PMM/balance centre, the location of the centre of gravity relative to ship origin O, the mass and inertia properties of the oscillating system, the time delay of the measured signals, the start time of the Fourier analysis (here taken to be one full cycle after the start of the motion), and the number of cycles over which Fourier analysis shall be conducted (here, three cycles). The option to correct for inertial forces was checked, so that the software would calculate the model inertial forces and moments and subtract them from the measured forces: Fourier analysis was therefore carried out directly on the pure hydrodynamic forces. This is further developed in Section 5.0.
7. Further analysis of the harmonic runs to derive hydrodynamic coefficients from this information will be conducted using either the analysis module "pmmana" or custom analysis workbooks in Excel.

The time delay of measured signals mentioned above stems from the fact that the harmonic run analysis program "pmmana" does not use measured signals for PMM velocities, but noise-free velocities from the prescribed motions as input to the PMM (velocities from the PMM drive signal files "vorg*yyyy*.csv"). Due to low-pass filtering applied to all measurements, there is a small time shift between the measured forces and the corresponding command velocities which are not measurements. The time shift depends on the signal conditioning, and an accurate estimate of it is crucial for correct determination of the out-of-phase components in the Fourier analysis that yield the added masses and added moments of inertia (acceleration derivative coefficients). The time shift was verified and corrected for each run in the following way, before carrying out step 5 above:

- Both measured and input PMM velocities were plotted against time for each run, and the time shift between them was visually determined and logged, to the closest hundredth of a second.
- The time shift was also later verified using Fourier analysis and corrected where necessary.

The time shift ranged between 0.15 and 0.27 seconds depending on the run. The variation is due to the process used for selecting the start time of analysis segments.

5.0 DETERMINATION OF HYDRODYNAMIC COEFFICIENTS

5.1 Equations of motion

General equations

The determination of hydrodynamic forces and moments from PMM tests proceeds from considering the equations of motion: Newton's second law is written for a well-chosen system.

In the case of a captive model, the chosen system is constituted of all parts below the load cells, so-called live parts. It includes the model and the live part of the balance, but not the ground part of the balance or the tow post. External forces applied to this system are it: its weight, a constant vertical force; forces exerted by the water onto the appended hull, both hydrostatic and hydrodynamic; and forces applied by the balance: these are the opposite forces measured by the balance load cells. We include within hydrodynamic forces those exerted by water onto the propeller and onto the hull due to propeller rotation.

In the case of the ship, the system is the full vessel. External forces applied are: its weight; and forces exerted by water, both hydrodynamic and hydrostatic.

Newton's second law is written for the system (S) in an inertial frame of reference, at ship origin O:

$$\begin{aligned} m\frac{d}{dt}\left(\vec{V}_O(S/Earth)\right) &= \sum \vec{F} \\ I_O\frac{d}{dt}\left(\vec{\Omega}(S/Earth)\right) &= \sum \vec{M}_O \end{aligned} \tag{8}$$

where I_O is the moment of inertia tensor at ship origin O.

Besides the inertial frame of reference, two local coordinate systems are considered:

- the ship-fixed coordinate system (O, x*, y*, z*) with x* positive forward, y* positive to starboard, and z* positive down.

- A hybrid coordinate system (O, x, y, z) attached partly to the ship: it follows the surge, sway, heave and yaw motions but not the pitch and roll motion of the ship: the x and y axis are horizontal, and the z axis is vertical.

The coordinate systems are illustrated in Figure 18, from Reference [16].

We define the motions of the ship in the hybrid system:

- u is the velocity at O, relative to Earth, in the x-direction.
- v is the velocity at O, relative to Earth, in the y-direction.
- φ is the rotation around the x-axis. (roll)
- ψ is the rotation around the z-axis. (yaw)
- The components of the angular velocity vector of the ship, expressed in the hybrid coordinate system are $p = \dot{\varphi}$, $q = \dot{\theta}$, and $r = \dot{\psi}$.
- The dots denote time derivatives.

The pitch and heave motions are small and are neglected. The x*-axis is then coincident with the x-axis.

The equations of motion of the ship or model, projected in the hybrid coordinate system become:

$$
\begin{gathered}
m[\dot{u} - rv - x_G^* r^2 + z_G^*(2rp\cos\varphi + \dot{r}\sin\varphi)] = X \\
m[\dot{v} + ru + x_G^*\dot{r} + z_G^*((r^2 + \dot{p}^2)\sin\varphi - \dot{p}\cos\varphi)] = Y \\
I_{xx}\dot{p} - I_{xz}\dot{r}\cos\varphi + (I_{zz} - I_{yy})r^2\sin\varphi\cos\varphi - mz_G^*\cos\varphi(\dot{v} + ur) = K \\
(I_{yy}\sin^2\varphi + I_{zz}\cos^2\varphi)\dot{r} + 2(I_{yy} - I_{zz})rp\sin\varphi\cos\varphi - \\
I_{xz}(\dot{p}\cos\varphi - p^2\sin\varphi) + mx_G^*(\dot{v} + ur) + mz_G^*\sin\varphi(\dot{u} - vr) = N
\end{gathered}
\tag{9}
$$

- m is the mass of the system (S) being considered.
- x^*_G and z^*_G are the coordinates in the ship-fixed coordinate system of the centre of gravity G of the system.
- Moments and products of inertia $I_{xx}, I_{yy}, I_{zz}, I_{xz}$ are defined about the ship-fixed axis through the ship origin O.
- X, Y, K, N here are the components in the hybrid coordinate system of the total external forces and moments at ship origin O.

Simplified equations for the case of controls-fixed stability:

In the case of our captive model tests for the study of controls-fixed stability, there is no roll actuation and heel angle φ is zero. Besides, the only two equations of interest are that along the y-axis and that around the z-axis.

We subtract from equations (9) at speed, the equations (9) at rest (during the tare segment of a run before the propeller is set to speed) when the balance reaction forces equal the sum of weight and hydrostatic forces. The second and fourth equations hence reduce to:

$$m[\dot{v} + ru + x_G^* \dot{r}] = Y_H - Y_B$$
$$(I_{zz}\dot{r} - + mx_G^*(\dot{v} + ur) = N_H - N_B \quad (10)$$

where:

Y_H, N_H are the hydrodynamic side force and yaw moment at O, and

Y_B, N_B are the tared reaction side force and yaw moment at O as measured by the balance (equal to the measured FY and MZ respectively, tared).

Therefore, the hydrodynamic forces at ship origin are calculated as the sum of the tared balance forces and the inertial forces:

$$Y_H = Y_B + m[\dot{v} + ru + x_G^* \dot{r}]$$
$$N_H = N_B + I_{zz}\dot{r} + mx_G^*(\dot{v} + ur) \quad (11)$$

For "static" runs (drift runs) the inertial terms are null: then the hydrodynamic forces are directly equal to the measured reaction forces of the balance with the tare removed.

For simplification of notation, from here on we will denote by Y, N the hydrodynamic side force and yaw moment at O, omitting the $_H$ subscript.

5.2 Non-dimensionalization

The non-dimensional form of a quantity *a* will be noted *a*'.

The characteristic scales used herein to non-dimensionalize the terms and equations are:

- Length: length between perpendiculars, noted L or Lpp. For the contract design of JSS, $L = 5.8714m$ at model scale.
- Time: L/U where U is the instantaneous model velocity along the track: $U = \sqrt{(u^2 + v^2)}$.

- Mass: $0.5\rho L^3$ where ρ is the water density; for these tests, the water temperature was 18.2 degree Celsius: $\rho = 998.6 kg.m^{-3}$.

We also define a reference velocity: U_{ref} corresponds to the approach speed, i.e. in this case the straight-line speed, speed at which ship self-propulsion is modelled. For our tests U_{ref} is the model speed corresponding to the full scale speed of 18 knots.

Non-dimensional magnitudes of hydrodynamic forces and moments are obtained by dividing forces by $0.5 * \rho U^2 L^2$ and moments by $0.5 * \rho U^2 L^3$. Non-dimensional side force is noted Y' and non-dimensional yaw moment noted N'.

All other quantities are made non-dimensional with proper products and powers of $\rho/2$, U and L:

- linear velocities (u, v) are divided by U
- linear accelerations are divided by U^2/L
- angular velocities are divided by U/L
- angular accelerations are divided by U^2/L^2
- masses are divided by $0.5 * \rho L^3$;
- moments of inertia and products of inertia are divided by $0.5 * \rho L^5$

Angles are in radians.

Rudder angle in non-dimensional form (in radians) will be interchangeably noted d or d'.

5.3 Mathematical model of forces and moments

The mathematical model adopted here to express the hydrodynamic forces and moments in terms of hydrodynamic coefficients, is the model as coded in the software provided by HSVA: this software is used at NRCSJS for analysing dynamic runs and inferring hydrodynamic coefficients, and for generating simulations. The model is a whole-ship, or Abkowitz type, model (see Reference [4]). It is based on a Taylor expansion of forces and moments around a straight-ahead equilibrium condition at approach speed U_{ref}, and it includes terms up to the third order.

For our current study we are only concerned with hydrodynamic coefficients for side force Y and yaw moment N.

The full non-linear model proposed is, in non-dimensional form and neglecting roll motion:

For non-dimensional side force Y':

$$\begin{aligned} Y' = {} & Y'_0 + Y'_d\, d + Y'_{ddd}\, d^3 + Y'_v\, v' + Y'_{vvv}\, v'^3 + Y'_{\dot{v}}\, \dot{v}' + Y'_r\, r' + Y'_{rrr}\, r'^3 + Y'_{\dot{r}}\, \dot{r}' \\ & + Y'_{vrr}\, v' r'^2 + Y'_{vvr}\, v'^2 r' + Y'_{vvd}\, v'^2 d + Y'_{vdd}\, v' d^2 \\ & + Y'_{rrd}\, r'^2 d + Y'_{rdd}\, r' d^2 + Y'_{vrd}\, v' r' d + Y'_{ud}\, d\Delta u' + Y'_{uddd}\, d^3 \Delta u' \end{aligned} \tag{12}$$

And the model for non-dimensional yaw moment N' follows the same expression where all Y notations are replaced by N notations.

Velocities u, v, r were defined in Section 5.1.
d is the rudder angle in radians.
Δu refers to $(u\text{-}U_{ref})$, made non-dimensional by dividing it like all other velocities by the instantaneous ship velocity along the track:

$$\Delta u' = (u - U_{ref})/U \tag{13}$$

The state variables in the above equations are in their non-dimensional form as defined in Section 5.2.

In Equation (12), Y'_o (and N'_o) are speed dependent due to the non-symmetry of the flow around the single-propeller ship.

In the case of controls-fixed stability tests, where the rudder angle is fixed at neutral angle, the simplified model becomes:

$$\begin{aligned} Y' = {} & Y'_0 + Y'_v\, v' + Y'_{vvv}\, v'^3 + Y'_{\dot{v}}\, \dot{v}' + Y'_r\, r' + Y'_{rrr}\, r'^3 + Y'_{\dot{r}}\, \dot{r}' \\ & + Y'_{vrr}\, v' r'^2 + Y'_{vvr}\, v'^2 r' \end{aligned} \tag{14}$$

(and the same model for N, with Y notations replaced by N notations.)

Further, in the case of a pure sway harmonic test (r=0):

$$\begin{aligned} Y' &= Y'_0 + Y'_v\, v' + Y'_{vvv}\, v'^3 + Y'_{\dot{v}}\, \dot{v}' \\ N' &= N'_0 + N'_v\, v' + N'_{vvv}\, v'^3 + N'_{\dot{v}}\, \dot{v}' \end{aligned} \tag{15}$$

And in the case of a pure yaw harmonic test (v=0):

$$\begin{aligned} Y' &= Y'_0 + Y'_r\, r' + Y'_{rrr}\, r'^3 + Y'_{\dot{r}}\, \dot{r}' \\ N' &= N'_0 + N'_r\, r' + N'_{rrr}\, r'^3 + N'_{\dot{r}}\, \dot{r}' \end{aligned} \tag{16}$$

Although we are only concerned with the linear coefficients to assess the directional stability, non-linear terms were present during the motions conducted with the PMM and must be considered in order to extract properly the linear terms.

In dimensional form, the model defining dimensional hydrodynamic coefficients is the same as written in equations (12) and (14), only without the prime notations.

5.4 Deriving Hydrodynamic Manoeuvring Coefficients from "static" runs

After pre-processing, further calculations were carried out on the data logged in the CSV file (see Section 4.7) using Excel. The components of the velocity vector at O in hybrid coordinates were calculated from carriage speed and from nominal yaw or drift angle ψ:

$$u = CarriageSpeed * \cos\psi \tag{17}$$

$$v = -CarriageSpeed * \sin\psi \tag{18}$$

The non-dimensional variables Δu', v' and d', and normalized forces and moments, were then computed per the formulas described in Sections 5.3 and 5.2.

All data extracted from static runs are presented in APPENDIX E: Static Tests: Table of Measured Data.

For drift tests with controls fixed, equations (15) and (16) become:

$$Y' = Y'_0 + Y'_v\, v' + Y'_{vvv}\, v'^3 \tag{19}$$

Y'_v (resp. N'_v) is obtained as the slope at the origin (v'=0) of the linear fit through the data of non-dimensional measured side force Y' (resp. yaw moment N') plotted against v'. The data is shown in Figure 19.

5.5 Deriving Hydrodynamic Manoeuvring Coefficients from harmonic runs

The harmonic runs were analyzed applying two methods: "multiple-run" harmonic analysis, and a further refined method performing direct multiple linear regression. Both methods make use to some degree of the analysis module ("pmmana") in the HSVA PMM software (or of equivalent calculations in Excel) for extracting harmonic (Fourier) coefficients up to the third order for the hydrodynamic forces and moments. The "pmmana" module collects and assembles run information, motion data and forces measurements, and determines Fourier coefficients.

The harmonic analysis method further relies on the pure harmonic nature of the motions, while the direct regression method does not make any assumptions about the motions (although it uses the periodic nature of the data to filter out the noise).

Fourier decomposition of forces and moments:

The non-dimensional measured hydrodynamic forces and moments are periodic functions. They are decomposed into third order truncated Fourier series:

$$F = \frac{a_{0F}}{2} + \sum_{k=1}^{3} a_{kF} \cos k\omega t + b_{kF} \sin k\omega t \tag{20}$$

where F is a general notation for either of the non-dimensional force X', Y' or moment K', N';
$a_{kF}, k = 1,3$ and $b_{kF}, k = 1,3$ are the Fourier coefficients for F(t).

Harmonic equations of motions

The development of harmonic equations is presented in dimensional form in Appendix F: Mathematical Model Equations in Harmonic Form, and in non-dimensional form in Appendix G: Non-Dimensional Equations Written in Harmonic Form.

Pure harmonic motions with rudder fixed at neutral angle can be described by the following set of equations:

$$\begin{aligned} &\text{Pure Sway}: v = v_a \cos(\omega t), r = 0 \\ &\text{Pure Yaw}: r = r_a \cos(\omega t), v = 0 \\ &u = u_0 \\ &d = \text{constant} \end{aligned} \tag{21}$$

(See Section 5.1 for the definition of velocities u, v, r; d designates the rudder angle in radians)

In non-dimensional form, the kinematic equations in harmonic notation, up to the first order, are:

$$\begin{aligned} u' &\approx u'_0 \\ \dot{u}' &= 0 \\ \text{Pure Sway}: v' &\approx v'_1 \cos \omega t \\ \dot{v}' &\approx \dot{v}'_1 \sin \omega t \\ r' &= 0 \\ \text{Pure Yaw}: r' &\approx r'_1 \cos \omega t \\ \dot{r}' &\approx \dot{r}'_1 \sin \omega t \\ v' &= 0 \end{aligned} \tag{22}$$

The expressions for non-dimensional amplitudes $v'_1, r'_1, \dot{v}'_1, \dot{r}'_1, u'_0$ are given in Appendix G: Non-Dimensional Equations Written in Harmonic Form.

Multiple-run harmonic analysis

In harmonic analysis, both sides of the mathematical model equation (14) are written in harmonic form: velocities and variables on the right-hand side are replaced by their harmonic expression (Equations 22), while the force/moment on the left-hand side is replaced by its third-order Fourier series expression (Equation 20). Identification of the harmonic components yields a set of equations, in which each force/moment Fourier coefficient a_{kF} is a polynomial function of the non-dimensional motion amplitudes v'_1, r'_1, u'_0, and the coefficients of the polynomial function are factors of the hydrodynamic coefficients.

For pure harmonic sway tests, the set of polynomial equations is:

$$\begin{aligned} \frac{a_{0Y}}{2} - a_{2Y} &= Y'_0 \\ a_{1Y} - 3a_{3Y} &= Y'_v v'_1 \\ a_{3Y} &= \frac{1}{4} Y'_{vvv} v'^3_1 \\ b_{1Y} &= Y'_{\dot{v}} \dot{v}_1 \end{aligned} \tag{23}$$

And for pure harmonic yaw tests:

$$\begin{aligned} \frac{a_{0Y}}{2} - a_{2Y} &= Y'_0 \\ a_{1Y} - 3a_{3Y} &= Y'_r r'_1 \\ a_{3Y} &= \frac{1}{4} Y'_{rrr} r'^3_1 \\ b_{1Y} &= Y'_{\dot{r}} \dot{r}'_1 \end{aligned} \tag{24}$$

(and equivalent sets of equations for non-dimensional yaw moment N', changing all Y notations to N notations).

In "multiple-run" harmonic analysis, coefficients in *v* and in *r* are determined as the slopes of a_1-$3a_3$ versus v'_1 and r'_1, respectively (second equation of sets (24) and (25)). Coefficients in $\dot{v}$ and in $\dot{r}$ are determined as the slopes of b_1 versus $\dot{v}_1$ and $\dot{r}_1$, respectively (fourth equation of sets (24) and (25)). A linear regression is performed on the set of data, for the full range of sway and yaw motion amplitudes tested.

The Fourier coefficients of non-dimensional side force and yaw moment for each harmonic run are presented in APPENDIX H: Harmonic Runs: Data Summary, along with the dimensional and non-dimensional parameters of the motion.

The data points from each run and the linear fit are plotted in Figures 20 to 22.

In practice we implemented the "multiple-run" analysis by using the solver in Excel for calculating the least squares regression line. The coefficients in *v* and in $\dot{v}$ were determined using the full set of pure sway harmonic runs, and the coefficients in *r* and in $\dot{r}$ were determined using the full set of pure yaw harmonic runs.

Direct multiple linear regression

The harmonic method of analysis above relies on the assumption that the motions have a known form and are purely harmonic motions, with only constant and first-order harmonics. But because carriage surge motion is disabled, during harmonic yaw motions carriage speed is constant and surge velocity is not. It follows that some amount of sway velocity and surge acceleration is present during harmonic yaw runs, which was not taken into account in Equations 21 to 25 above.

Using the harmonic analysis for the yaw tests therefore induces an error in the determination of the hydrodynamic coefficients in *r*, especially Y_r: a portion of the force is induced by the sway and surge motions and gets wrongly attributed to yaw rate. The parasitic sway motion during a harmonic yaw run is of small amplitude relative to the yaw motion, but because the side force hydrodynamic coefficient in sway (Y_v) is an order of magnitude larger than the side force hydrodynamic coefficients in yaw (Y_r), even a small amount of sway motion can generate a non-negligible hydrodynamic side force. Meanwhile, yaw moment which is the most important component of forces and moments generated by yaw rate is not affected greatly by the parasitic sway and surge motions present during harmonic yaw runs.

Therefore, in a second phase of analysis, a direct multiple linear regression method was applied to derive the correct hydrodynamic coefficients in *r*.

In the direct multiple linear regression method, no harmonic form is assumed for velocities and accelerations: they are calculated and considered at each point of time, using for motions the noise-free signals as input to the PMM. The periodic nature of the motions is used and the periodic time series of hydrodynamic forces and moments are still represented by their third-order Fourier series function at each point of time, as a means to filter the measurement noise in the forces.

The multiple linear regression analysis solves for the set of coefficients in the mathematical model equations (14) (in the present case we neglect the cross terms in *v* times *r*). The regression is performed over the whole set of data points in time, using all harmonic runs of all amplitudes.

The independent variables of the regression are the third-order Fourier series of the hydrodynamic forces and moments, which are time functions. The dependent variables are monomials of the motions (velocities, accelerations). The parameters of the regression are the non-dimensional hydrodynamic coefficients.

The direct linear regression method was implemented in Excel, making use of the solver tool. We applied this method for extracting the hydrodynamic coefficients in yaw from the full set of yaw harmonic runs, after the sway coefficients were determined either from static drift tests or from the full set of harmonic sway tests through direct regression.

5.6 Evaluation of the stability criterion C and of the stability index σ_1

Once a set of hydrodynamic coefficients was determined for a vessel configuration using a given method, the non-dimensional stability criterion C' and stability index σ_1 for that vessel configuration were calculated using formulas (5) and (4). The mass and moment of inertia for the full-scale ship are given in Table 9.

6.0 RESULTS

The hydrodynamic coefficients extracted from static tests (drift tests) are presented in Table 10. Plots of side force and yaw moment from which the linear coefficients were extracted are presented in Figure 19.

The multiple-run harmonic analysis is illustrated in Figures 20 to 22: the hydrodynamic coefficients are obtained as the slopes of a linear fit to the Fourier coefficients or combinations thereof. Although some scatter in the data and some departure from linearity are observed, overall the changes in hydrodynamic coefficients between vessel configurations are noticeable. The data for determination of Y_v and Y_r shows the most departure from linearity, therefore a second determination of these two coefficients was done, discarding the two runs of highest motion amplitudes. The resulting coefficients are presented in Table 11 for both the full set - using all runs, top table - and for the reduced set - discarding high amplitude motions, bottom table -. The Y_v coefficients determined over the lower amplitude motions are in better agreement with those extracted from the drift tests: the Y_v coefficients in the top table are high, which appears to skew the value of the stability criterion towards the positive side. The results for the JSS Preliminary Design applying the same harmonic analysis method to the January 2012 test data are shown for comparison.

Lastly, the hydrodynamic coefficients obtained from the direct linear regression are presented in Table 12. In the left-hand side of the table, coefficients in v were obtained from the drift tests and coefficients in vdot from the full set of harmonic sway tests, then the direct regression method was applied over the set of harmonic yaw tests to determine the coefficients in r and rdot. In the right-hand side of the table, coefficients in v and in vdot were obtained from applying direct regression through all harmonic sway tests, and then coefficients in r and rdot were determined by direct regression through the full set of harmonic yaw runs. The results are not significantly changed by the choice of using drift tests versus sway harmonic tests. The results for the JSS Preliminary Design applying the same method to the January 2012 test data are also shown for comparison. The regression fit through the times series data is illustrated for the JSS contract design configuration (with design rudder) in Figures 23 and 24 (for the hydrodynamic coefficients presented in the left-hand side of the table).

Results in Table 12 (left-hand side) are the final results for values of the hydrodynamic coefficients and stability criterion and index for the JSS Contract Design, and configuration variations.

7.0 DISCUSSION

The stability criterion and index are very sensitive to small variations in the determination of values of the hydrodynamic coefficients. The determination of the hydrodynamic coefficients carries uncertainty due to both the analysis procedure and the experimental setup, and so do the values of the stability criterion and the stability index.

The magnitude of uncertainty due to experimental error is indicated by the variation in results when repeating the test matrix for the JSS Contract Design configuration: as can be seen in Table 10 or Table 11, this variation is small relative to the change due to a different vessel configuration.

Different analysis methods for the extraction of hydrodynamic coefficients were tried and assessed carefully, and the final results for the hydrodynamic coefficients and the stability index of the JSS Contract Design are those obtained with the direct regression analysis method, results found in Table 12 and summarized here.

Configuration	JSS contract design (average of both tests)	JSS contract design, with Rudder 3	JSS contract design, with Rudder 2	JSS preliminary design (Jan 2012 tests)
Rudder	design rudder	Rudder 3	Rudder 2	design rudder
Y'v *1000	-11.53	-11.46	-12.18	-8.95
N'r *1000	-2.10	-2.18	-2.23	-1.90
Y'r *1000	2.51	2.66	2.81	2.33
N'v *1000	-4.94	-4.92	-4.92	-4.66
Y'vdot *1000	-10.42	-10.40	-10.49	-9.14
N'rdot *1000	-0.57	-0.54	-0.49	-0.49
A' *10^6	20.22	19.57	18.78	17.55
B' *10^6	52.68	53.68	55.20	43.12
C' *10^6	-7.7	-6.0	-3.0	-13.7
sigma1	0.14	0.11	0.05	0.29

The JSS Contract Design appears to be unstable, although a clear improvement was achieved over the Preliminary Design towards stability.

The tests with larger rudders show that the stability can be further improved significantly through the use of larger appendages. Importantly, the positive effect on stability of larger rudders was clearly demonstrated independently of the analysis method used.

Results from the January tests conducted on the Preliminary Design of JSS and with other appendage configurations can be found in Appendix I: Single-Run Method of Harmonic Analysis. These tests were analyzed using a harmonic method, developed as well in Appendix I. Although flaws have since been found in that analysis method and the resulting stability indices must be considered biased, those results are presented as they show the relative ranking of the different vessel configurations tested in both test sessions, with the Preliminary Design and the Contract Design.

It should be noted that the stability index derived from the tank testing also could carry error due to scale effects. This error is of unknown magnitude until the results of full

scale trials for this vessel will be available, but the choice of a relatively large model scale and the use of ship self-propulsion shaft speed in captive tests should help limit the scale effect.

8.0 REFERENCES

[1] Web Site: http://www.materiel.forces.gc.ca/en/jss.page, July 2010.

[2] "Principles of Naval Architecture", Volume III, Chapter IX Controllability, Section 4: "Analysis of Coursekeeping and Controls-Fixed Stability", Edward V. Lewis, 1988.

[3] Description of NRCSJS Towing Tank: http://www.nrc-cnrc.gc.ca/eng/facilities/iot/towing-tank.html , December 2009.

[4] Abkowitz, M.A., "Lectures on Ship Hydrodynamics-Steering and Manoeuvrability", Report No. Hy-5, Copenhagen, Denmark (1964).

[5] "General Description and Operating Manual of IOT PMM", Cussons Technology Ltd., February 2009 (draft).

[6] "Construction of Models of Ships, Offshore Structures, and Propellers", IOT Standard Test Method GM-1, V10.0, October 18, 2007.

[7] "Model Test Co-ordinate System & Units of Measure", IOT Standard Test Method GM-5, V6.0, November 29, 2004.

[8] Institute for Ocean Technology Work Instruction: "K&R Model Propulsion Dyno Calibration", FAC-24.

[9] "Data Acquisition, Verification and Storage", IOT Standard Test Method GM-2, V1.0, January 20, 2000.

[10] "Prediction of Ship Powering", IOT Standard Test Method TM-4, V4.0, December 12, 2006.

[11] ITTC Recommended Procedure and Guidelines: "Testing and Extrapolation Methods: Manoeuvrability: Captive Model Test Procedures", 7.5-02-06-02, Revision 02, 2008.

[12] "Model Propulsion in Open Water", IOT Standard Test Method TM-3, V6.0, December 12, 2006.

[13] Institute for Ocean Technology Standard Test Method: "Open Water Manoeuvring on the Planar Motion Mechanism PMM", VD1, 42-8595-S / TM-17, publication pending.

[14] Mills, Jason. GDAC DAQ File Format Version 2, LM-2012-01, NRC-IOT, December, 2011.

[15] Web Site: http://sweet.iit.nrc.ca/sweet/HomeSweetHome, September 2009.

[16] "Software Package for a new PMM – Cussons Project PMM for IOT", HSVA Report, January 2009.

[17] Comments on JSS Directional Stability, email note by Rob Pallard, 27 January 2012.

FIGURES

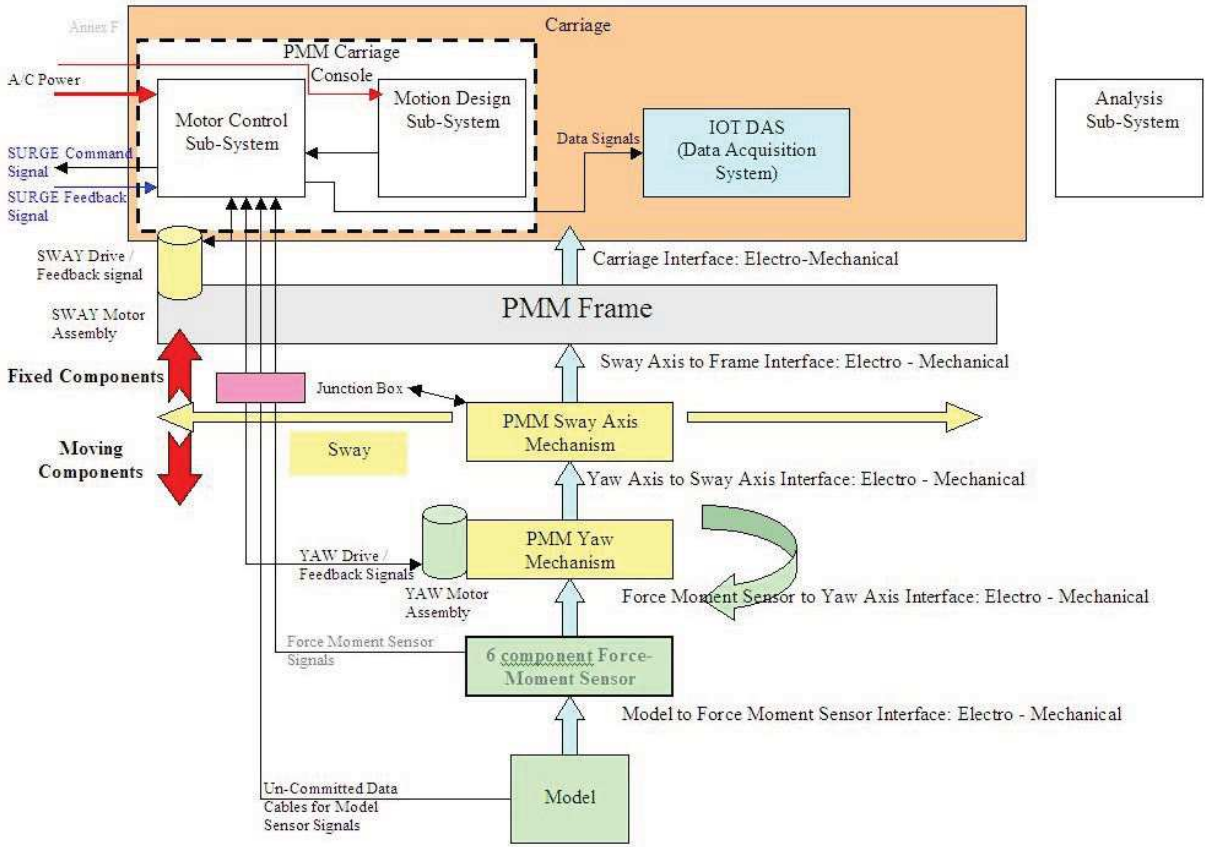

Figure 1. Planar Motion Mechanism Schematic

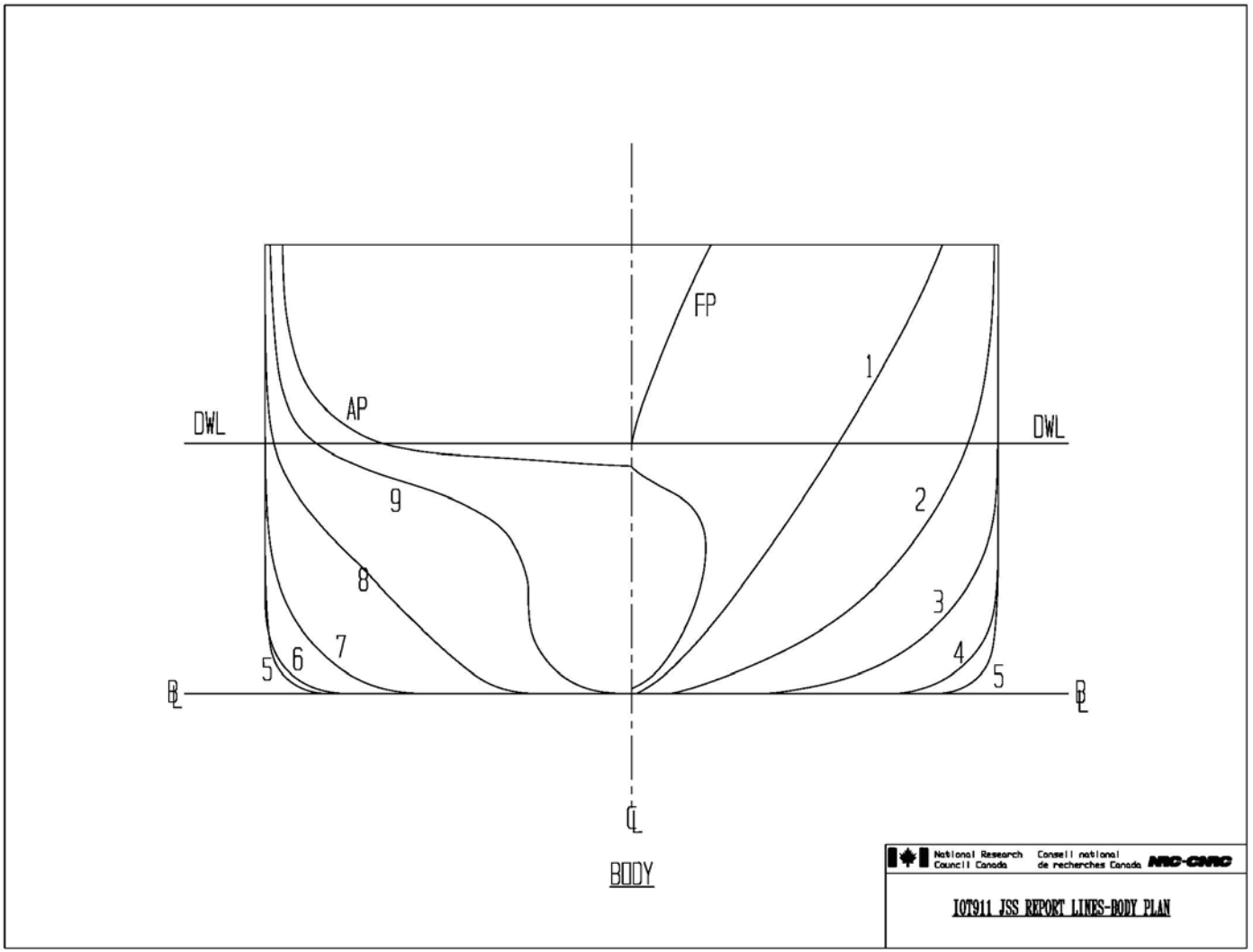

Figure 2. Model 911 – Body Plan

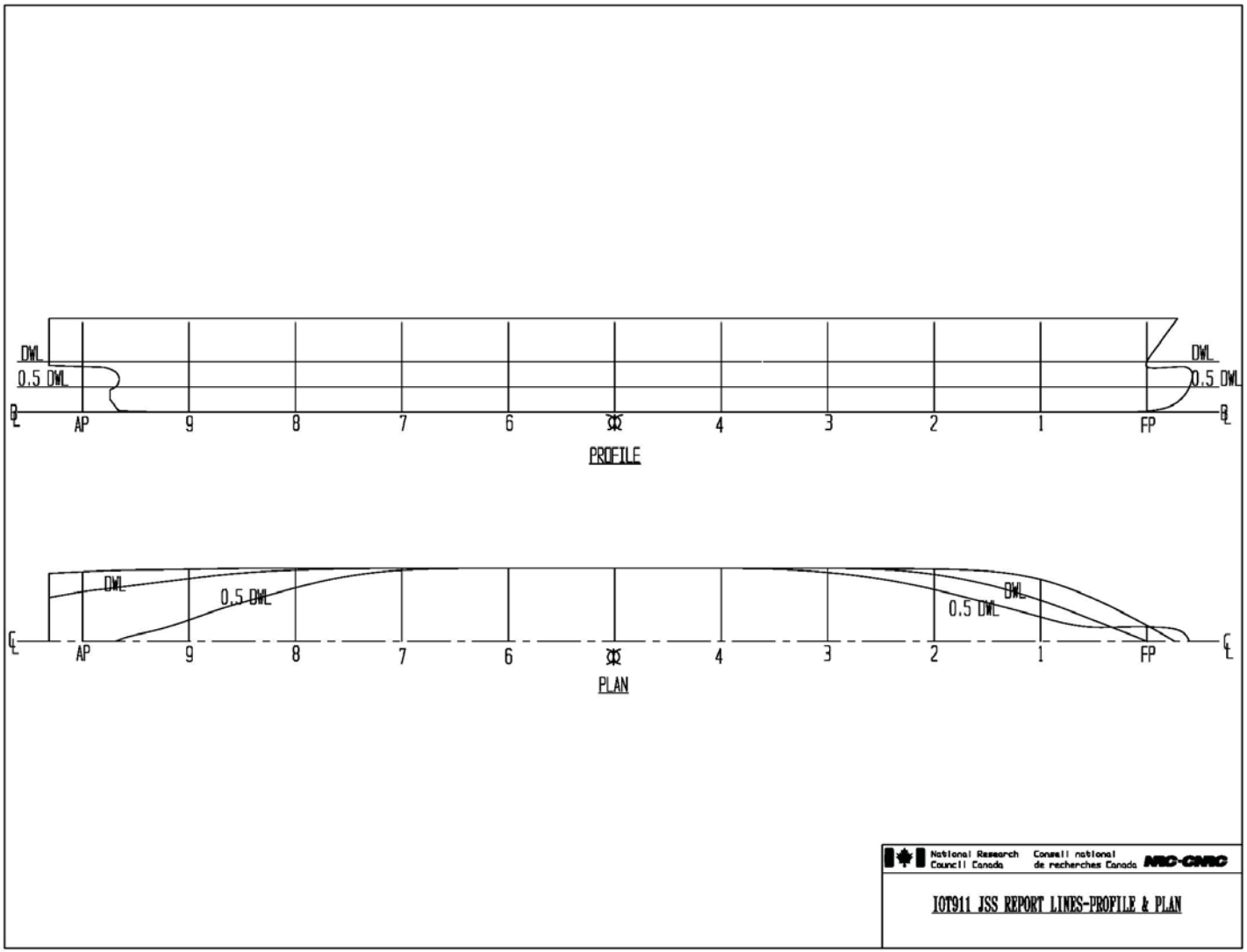

Figure 3. Model 911 – Profile and Plan

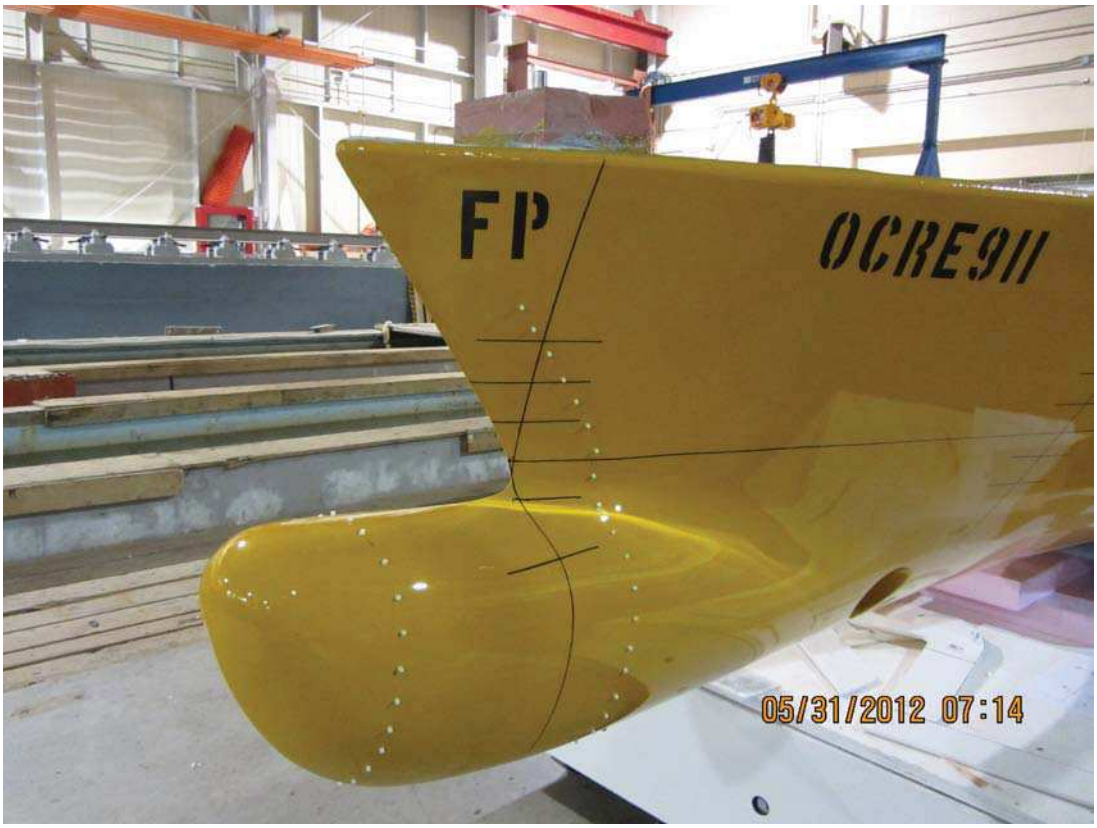

Figure 4. Model 911 – Turbulence Stimulation

Figure 5. Model 911 – Bow Thruster Tunnel

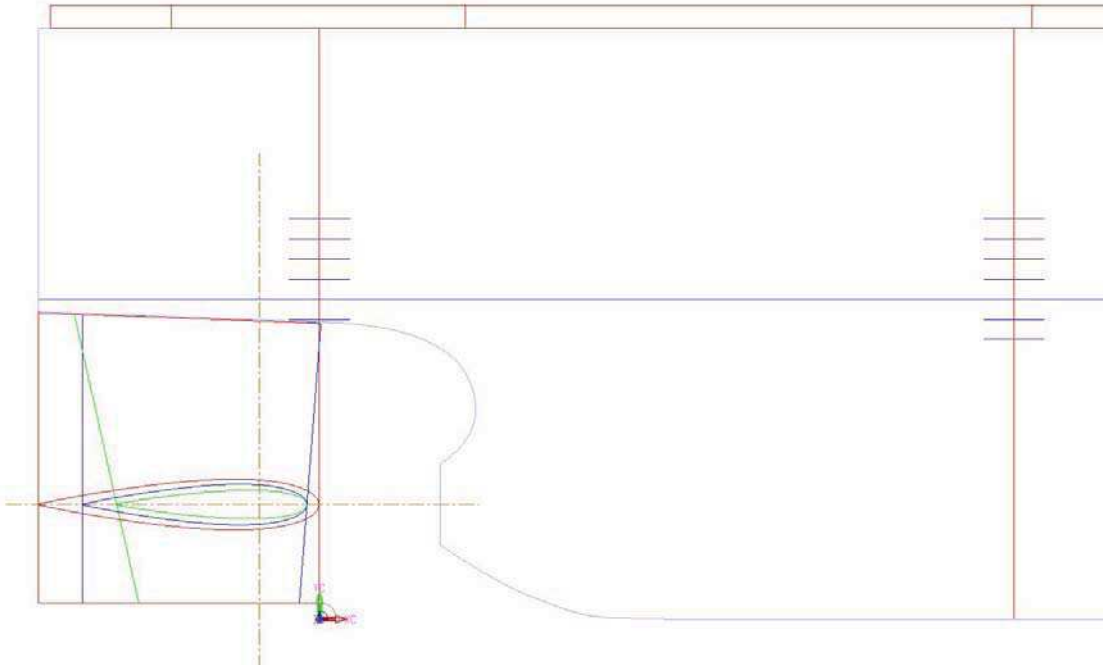

Figure 6. Comparison of Rudder 3 (blue) and Rudder 2 (red) with the design rudder (green)

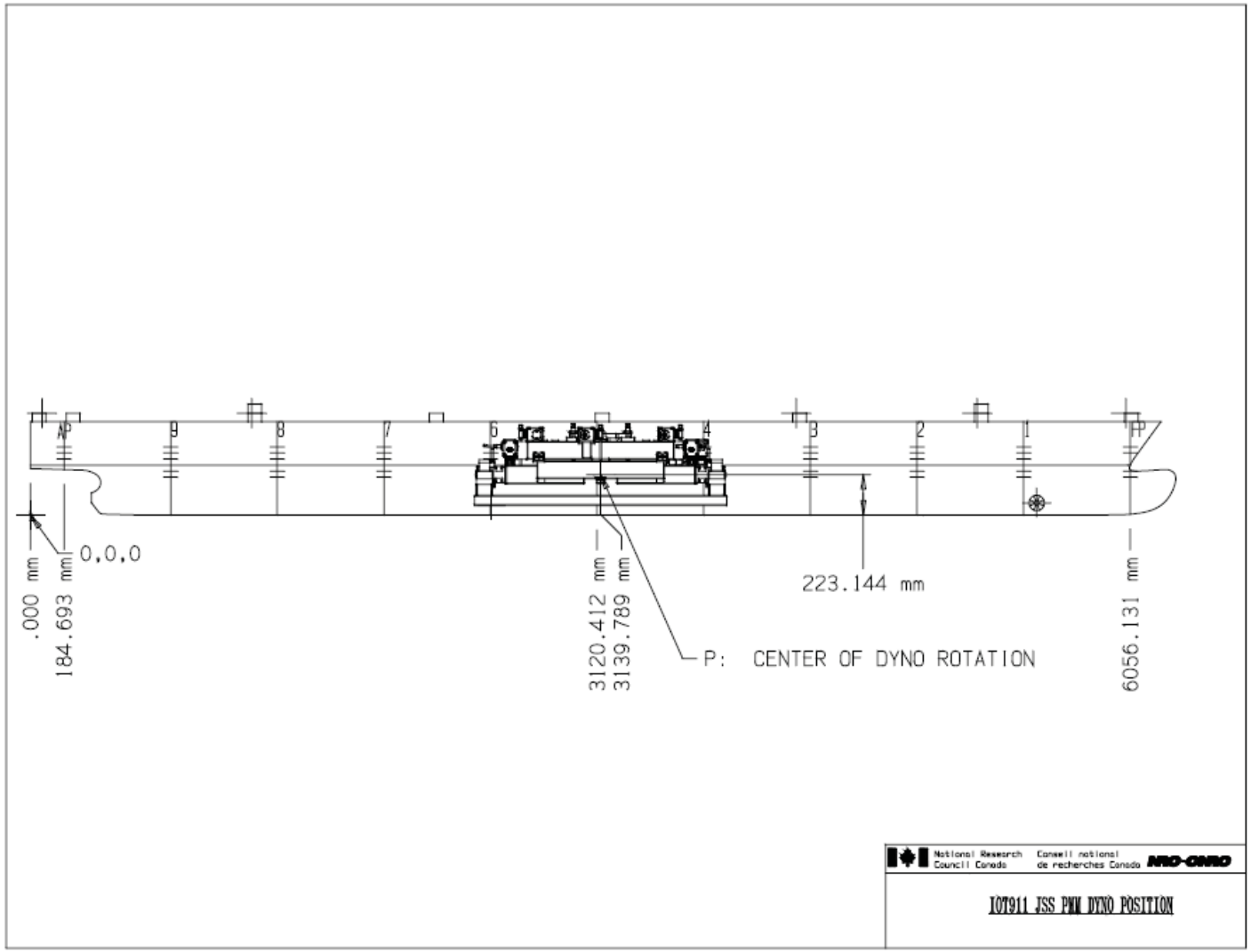

Figure 7. Model 911 – Position of PMM Force Balance

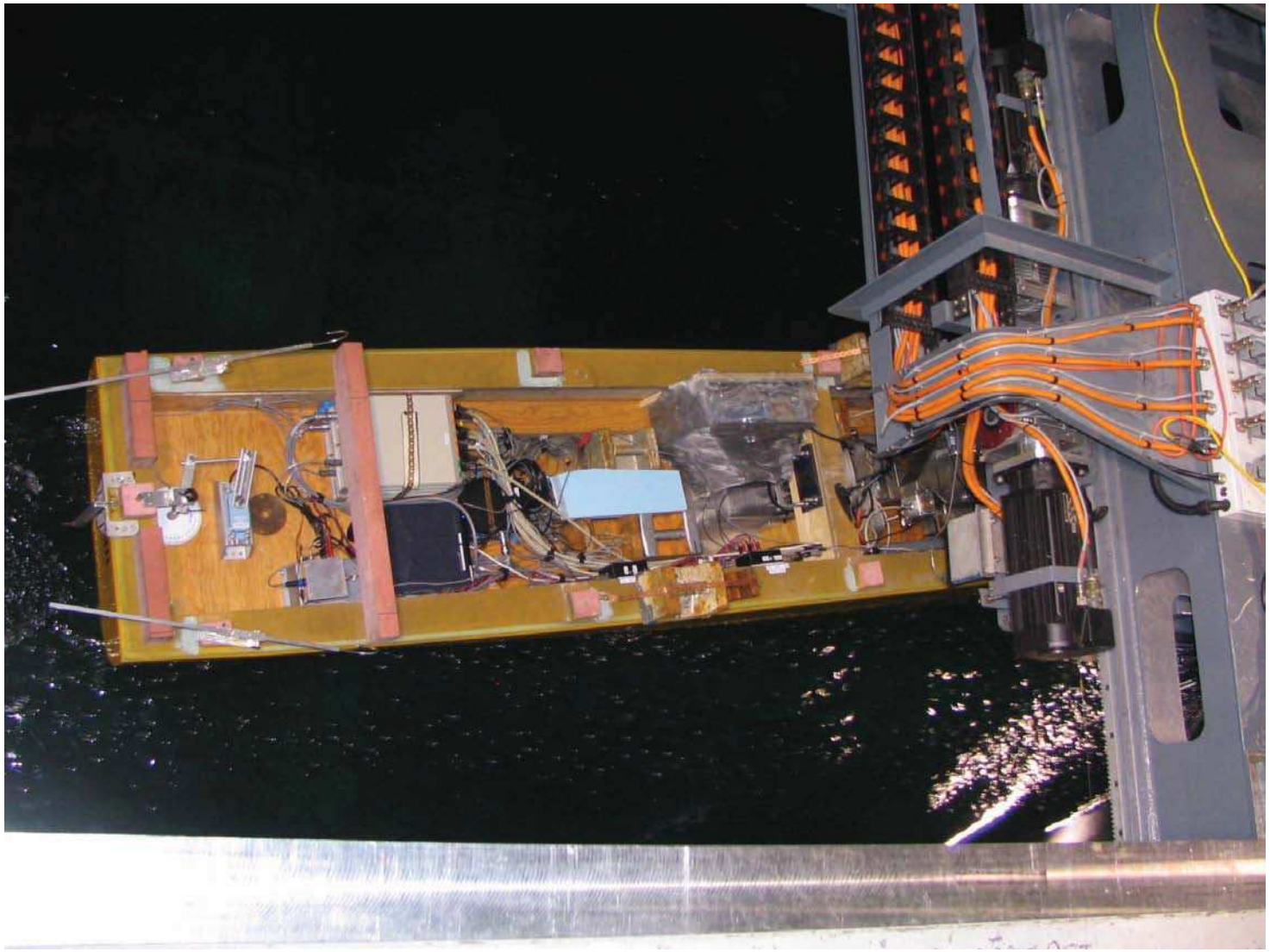

Figure 8. Stern of model 911 attached to the PMM, and instrumentation

Figure 9. Bow of model 911 attached to the PMM

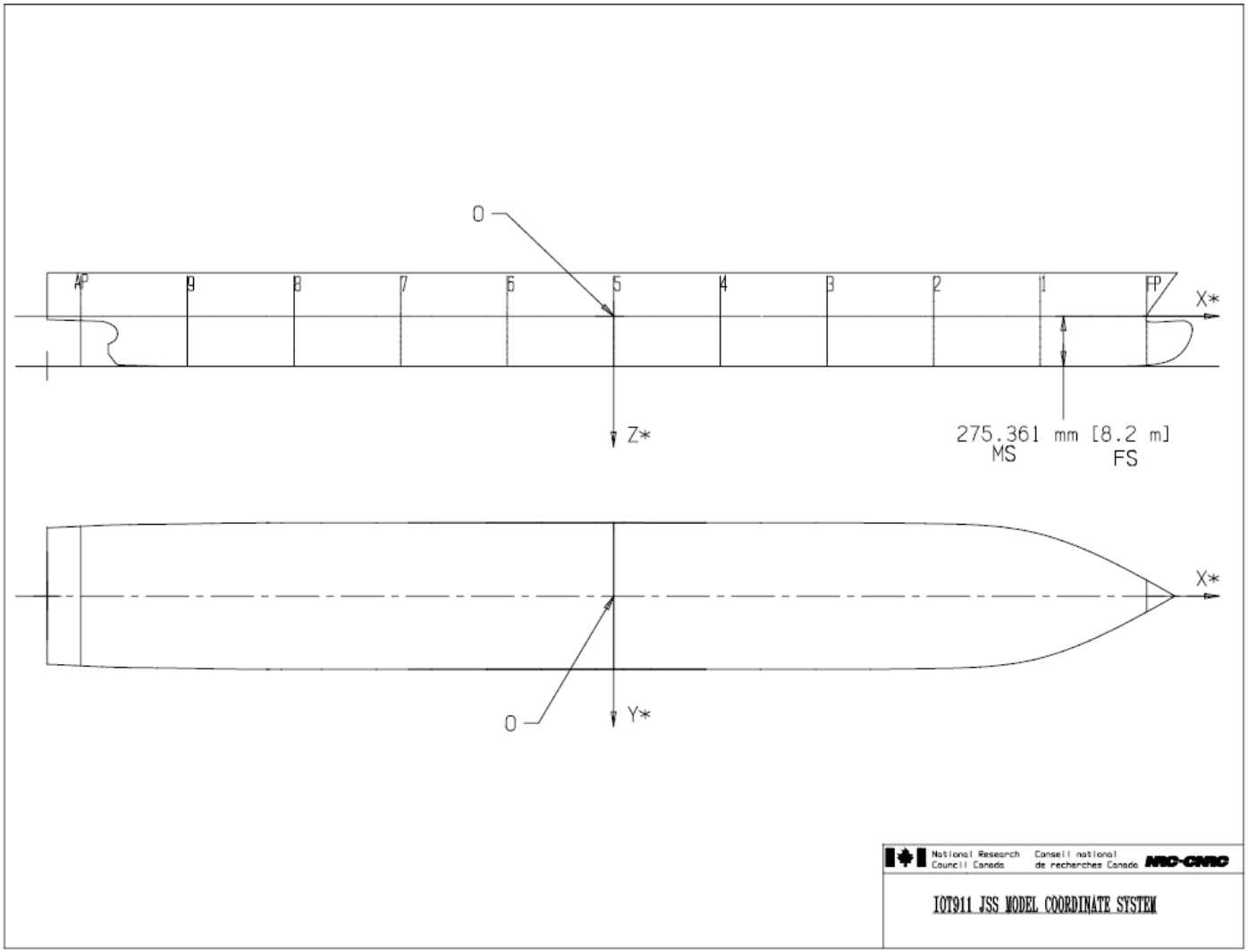

Figure 10. Model 911 – Model/Ship Origin and Coordinate System for Manoeuvring

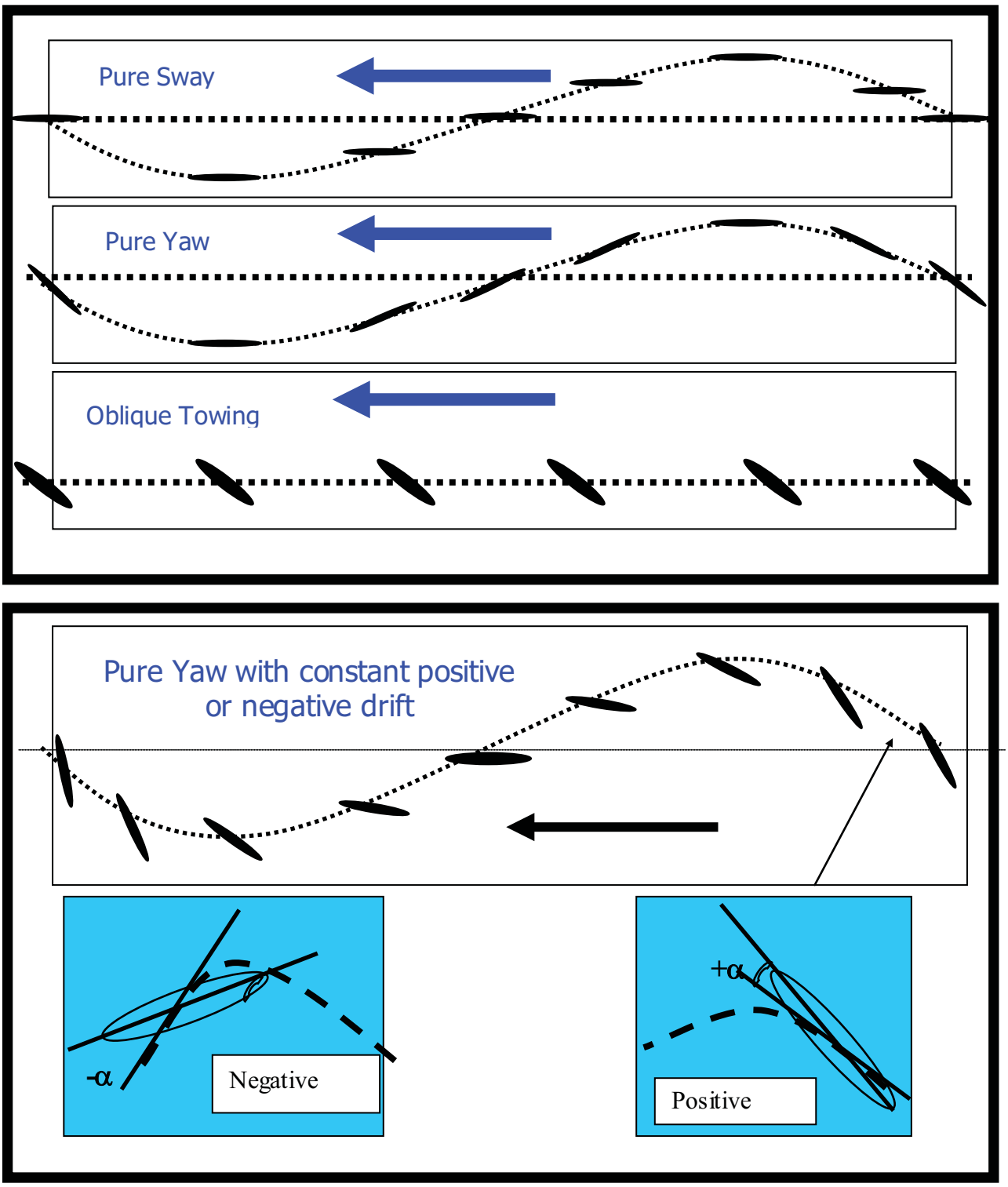

Figure 11. Vector Profiles for Typical PMM Manoeuvres

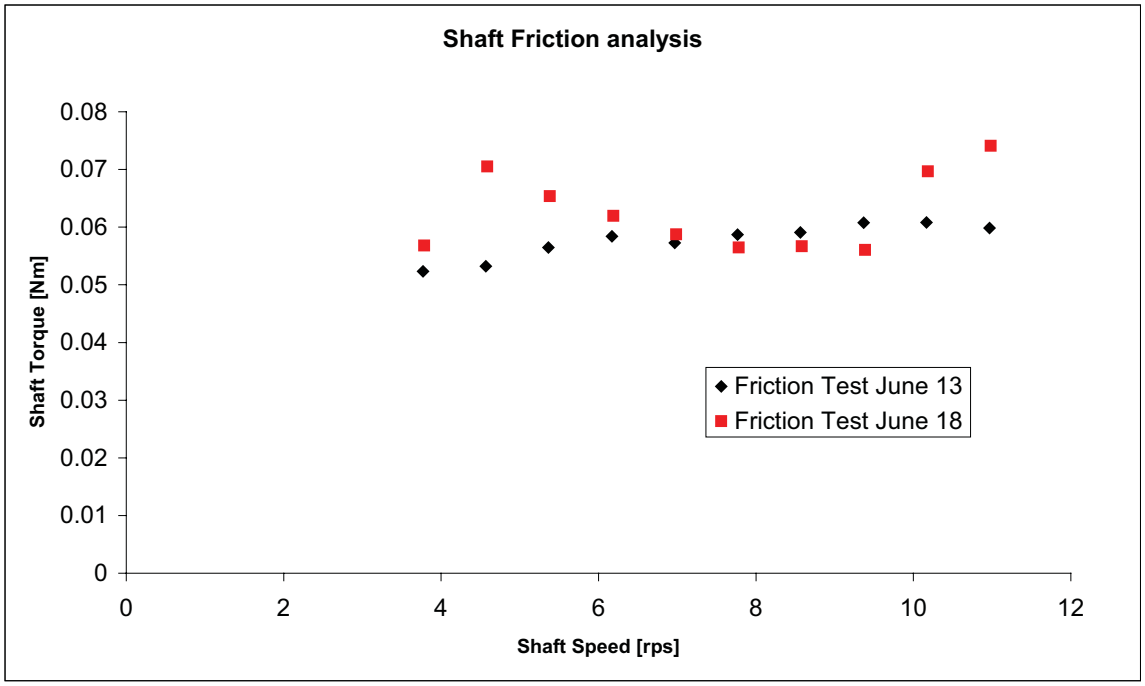

Figure 12. Results of Shaft Friction Tests

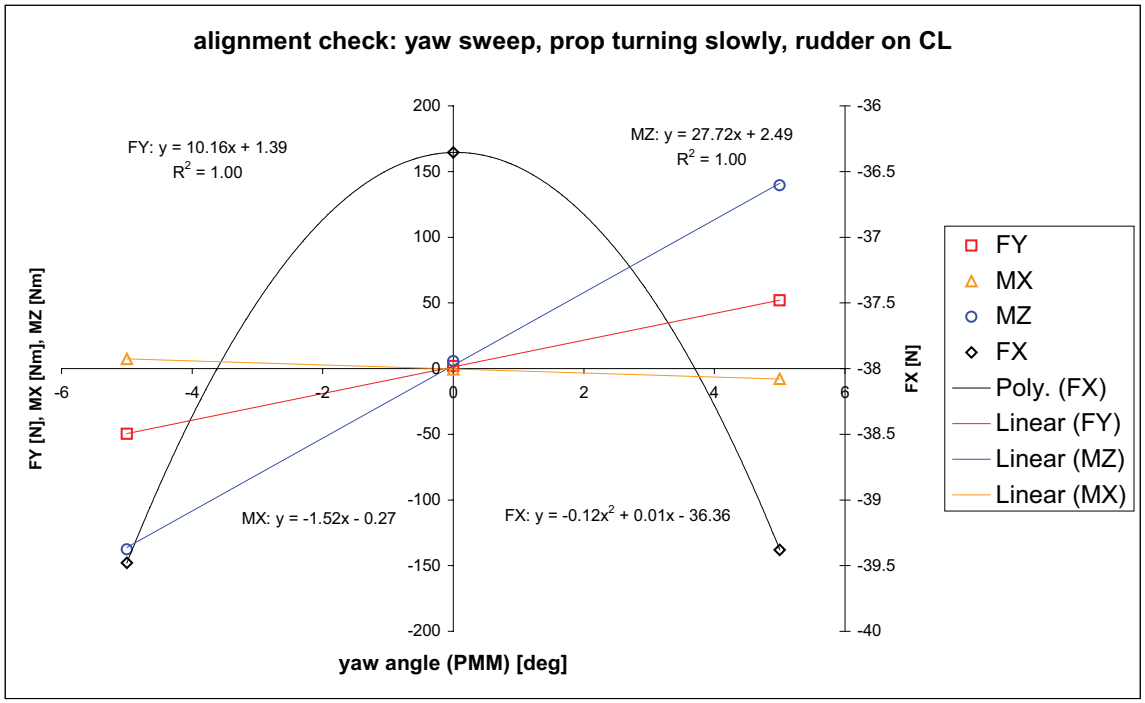

Figure 13. Result of Model Alignment Runs

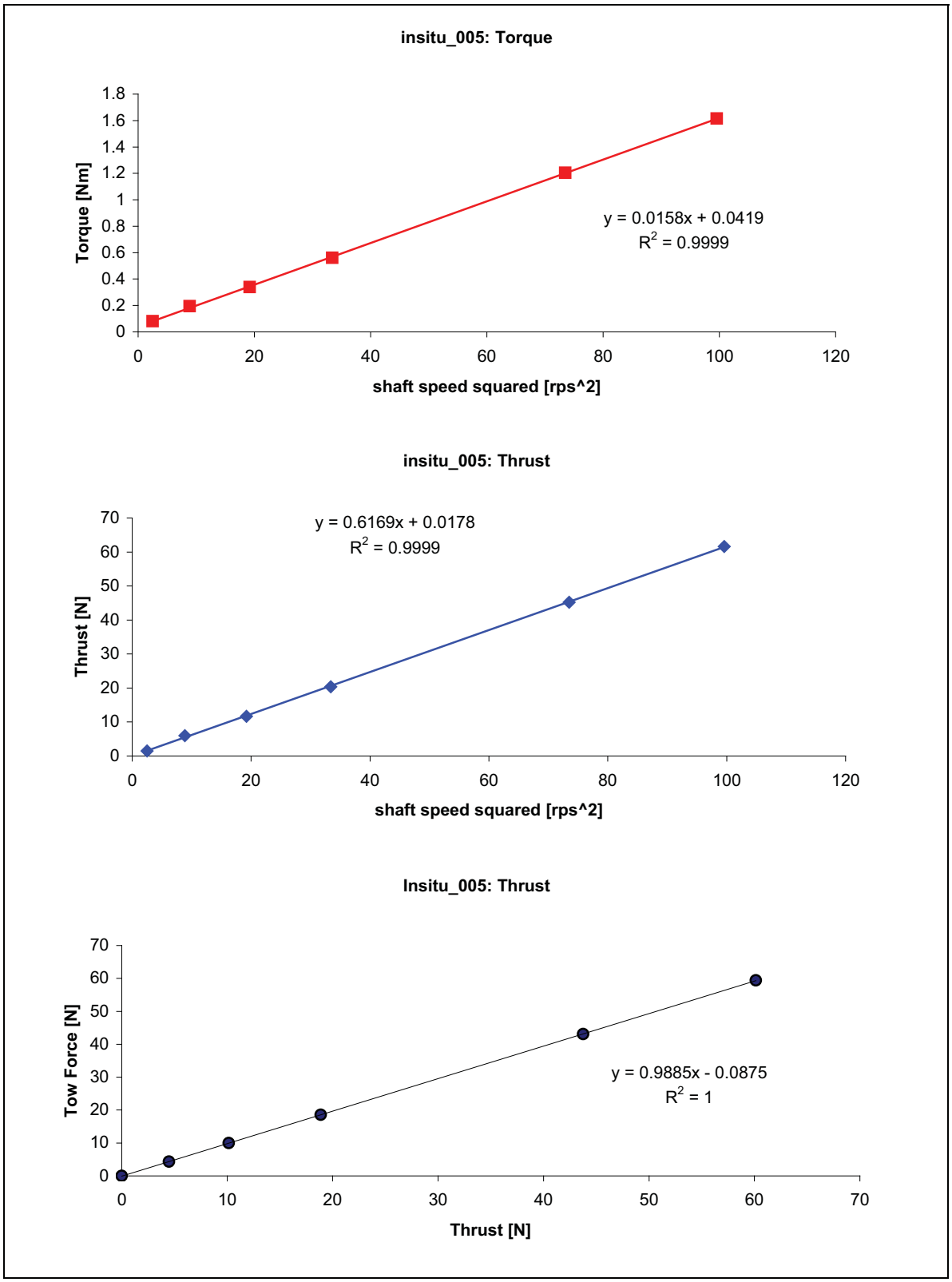

Figure 14. Example of Analysis of In-Situ Test

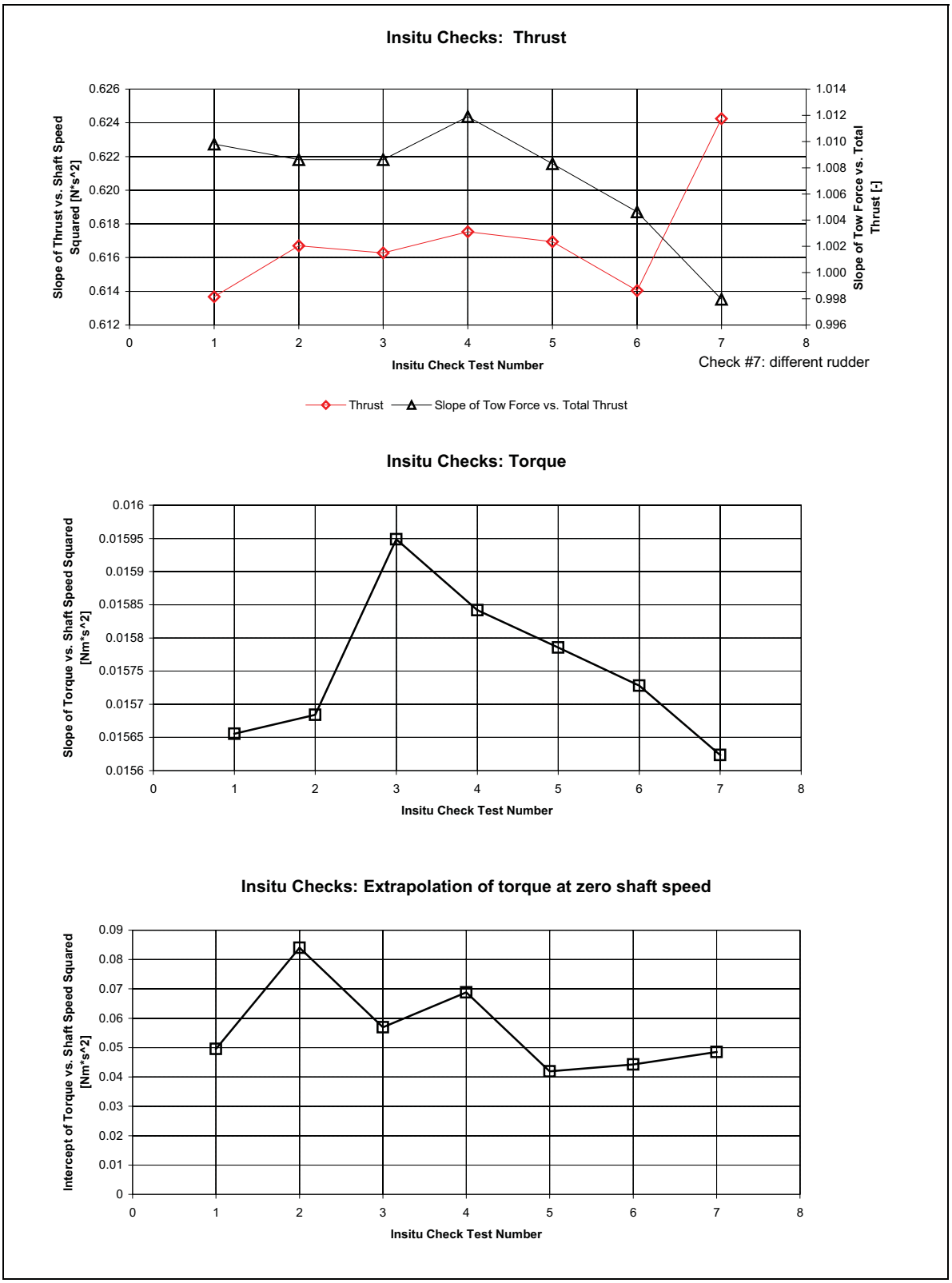

Figure 15. Summary of Results of all In-Situ Tests

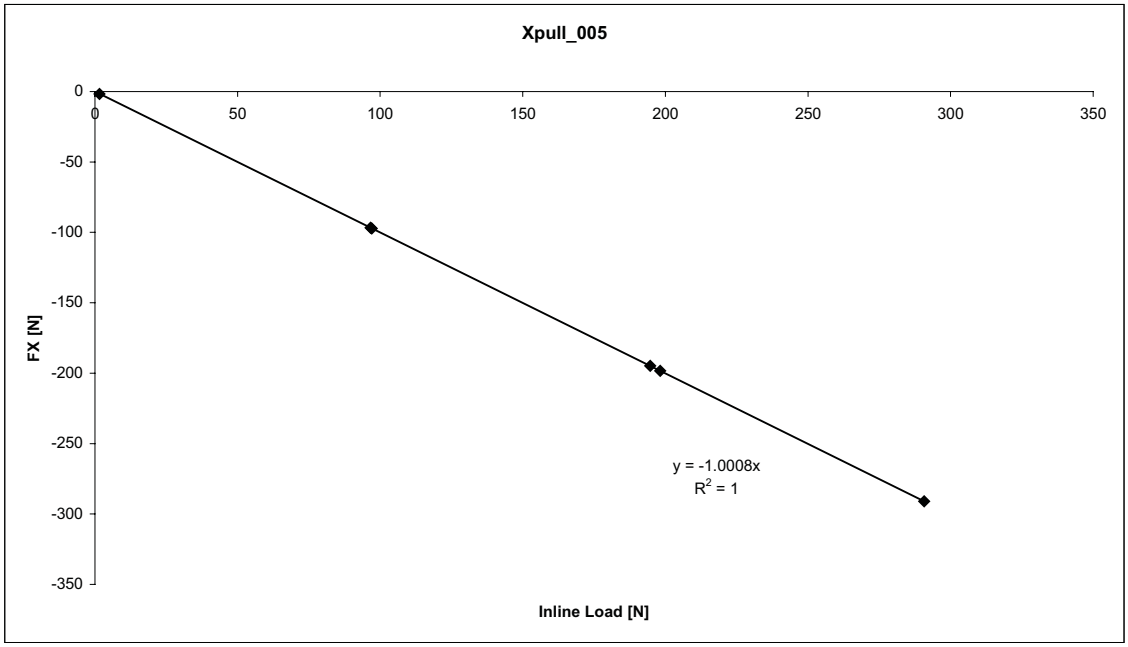

Pull	Slope	R-square	Change in slope
Xpull_PMM_001	-1.0010	1.0000	
Xpull_PMM_002	-1.0008	1.0000	-0.03%
Xpull_PMM_003	-1.0008	1.0000	-0.02%
Xpull_PMM_004	-1.0009	1.0000	-0.01%
Xpull_PMM_005	-1.0009	1.0000	-0.02%
Xpull_PMM_006	-1.0004	1.0000	-0.07%
Xpull_PMM_007	-1.0005	1.0000	-0.05%

Figure 16. Balance Longitudinal Pulls: Example Analysis Plot and Result Summary

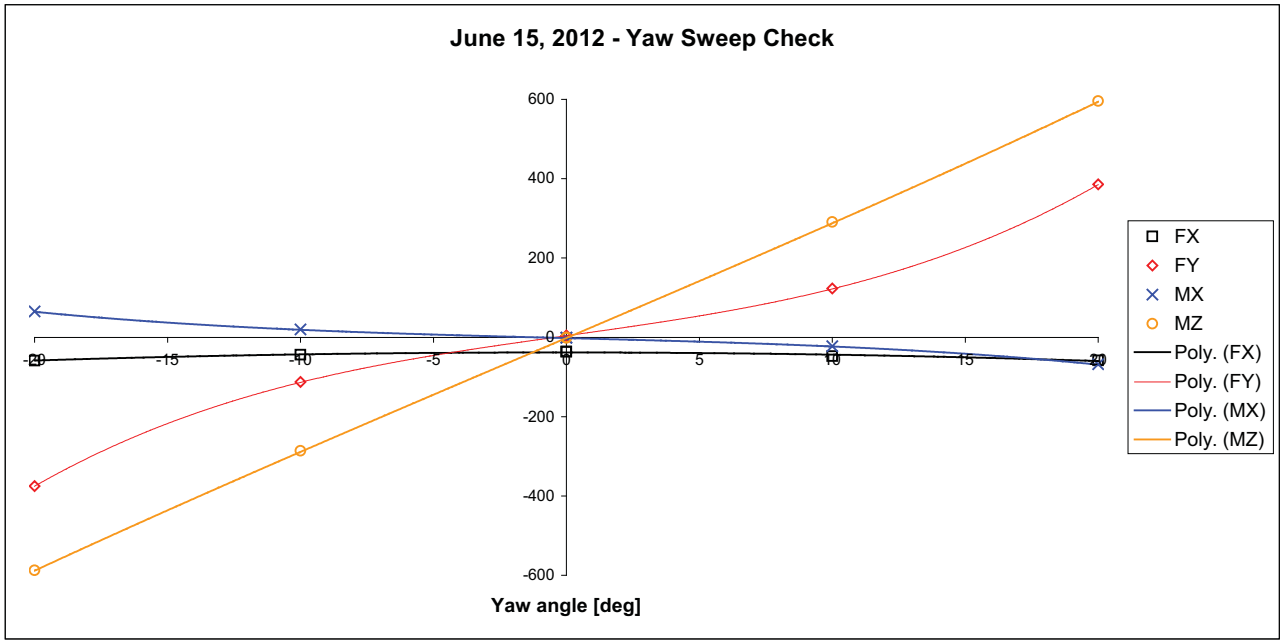

Date	FX			FY				MX				MZ				Rudder
	Intercept N	2nd order N/deg^2	R^2 -	Intercept N	1st order N/deg	3rd order N/deg^3	R^2 -	Intercept N	1st order N/deg	3rd order N/deg^3	R^2 -	Intercept N	1st order N/deg	3rd order N/deg^3	R^2 -	
13-Jun-12	-37.4	-0.0564	0.942	2.1	9.352	0.0254	1.0000	-0.4	-1.666	-0.0043	0.9999	-2.6	28.549	0.0050	1.0000	1 (design)
14-Jun-12	-37.7	-0.0558	0.941	2.5	9.677	0.0241	1.0000	-0.2	-1.759	-0.0041	0.9999	0.8	28.581	0.0037	1.0000	1 (design)
15-Jun-12	-37.9	-0.0525	0.945	5.1	9.382	0.0241	1.0000	-1.0	-1.684	-0.0041	1.0000	1.7	28.595	0.0025	1.0000	1 (design)
18-Jun-12	-38.4	-0.0544	0.937	3.7	9.558	0.0243	1.0000	-0.5	-1.704	-0.0042	0.9999	-0.2	28.772	0.0029	1.0000	1 (design)
9-Jul-12	-38.1	-0.0562	0.935	-7.7	9.651	0.0244	0.9976	1.6	-1.753	-0.0040	0.9976	-11.6	28.032	0.0054	0.9987	1 (design)
10-Jul-12	-37.7	-0.0583	0.952	-1.3	9.408	0.0252	0.9997	-0.3	-1.659	-0.0043	0.9997	8.0	28.189	0.0053	0.9999	1 (design)
11-Jul-12	-37.3	-0.0571	0.947	2.1	9.558	0.0251	0.9999	-0.2	-1.667	-0.0043	0.9999	-0.4	27.669	0.0037	1.0000	Rudder 3

Figure 17. Yaw Sweep Runs: Example Analysis Plot and Result Summary

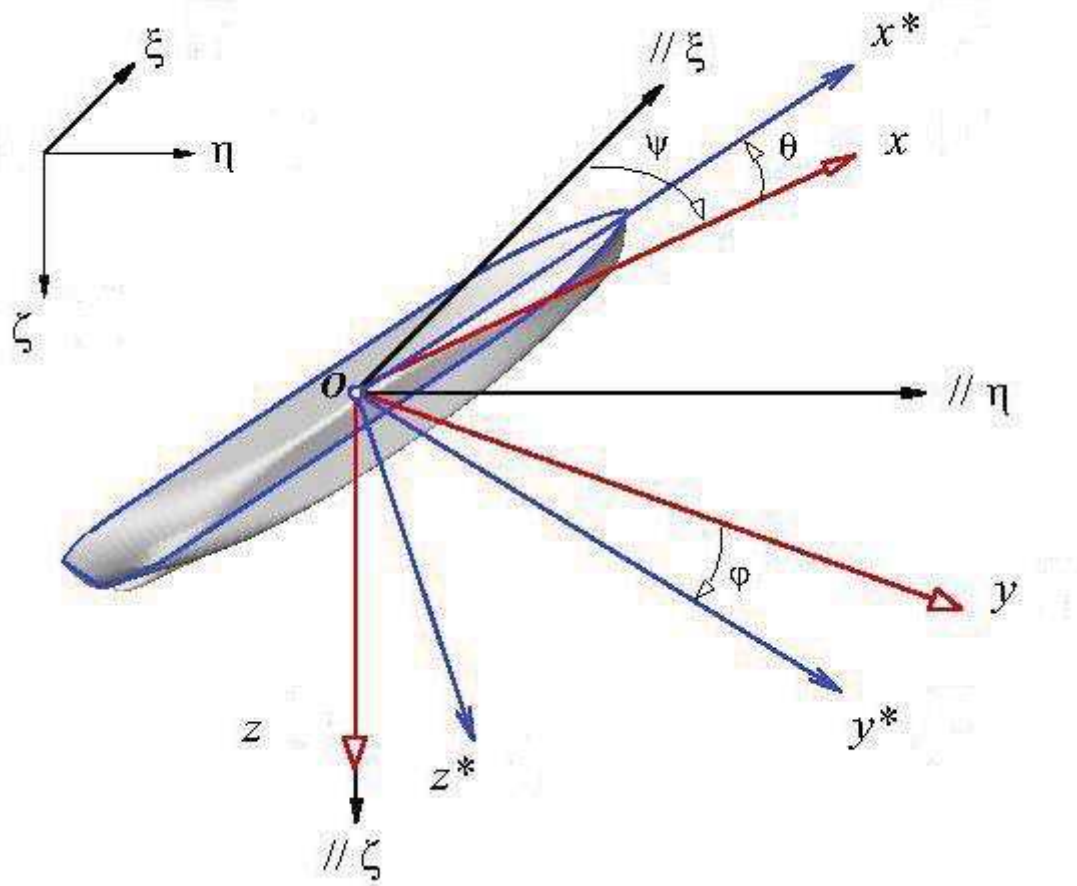

Figure 18. Earth-fixed (black), ship-fixed (blue) and hybrid (red) coordinate systems (Reference [15])

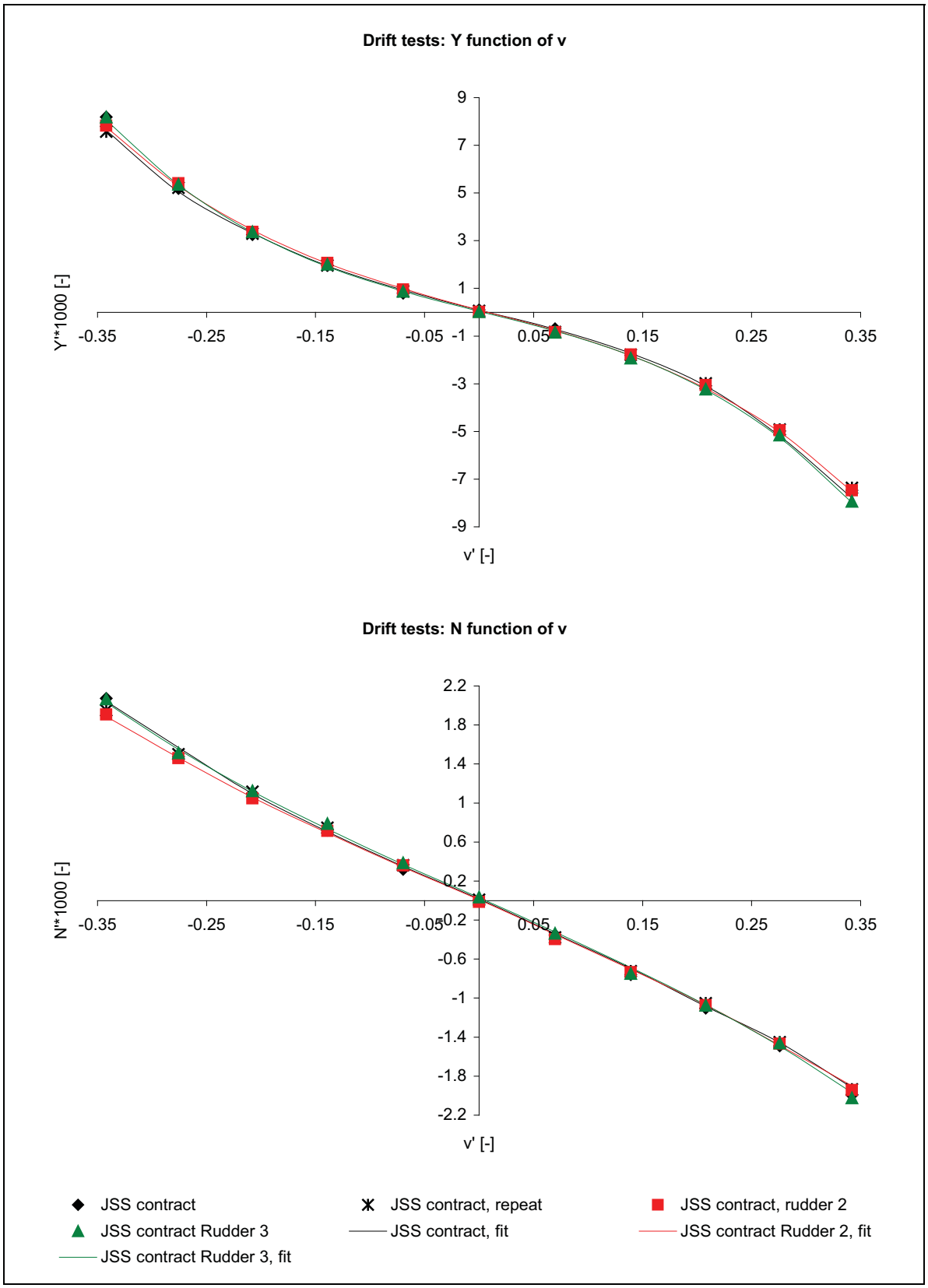

Figure 19. Non-dimensional Side Force and Yaw Moment Measured in Static Drift Tests

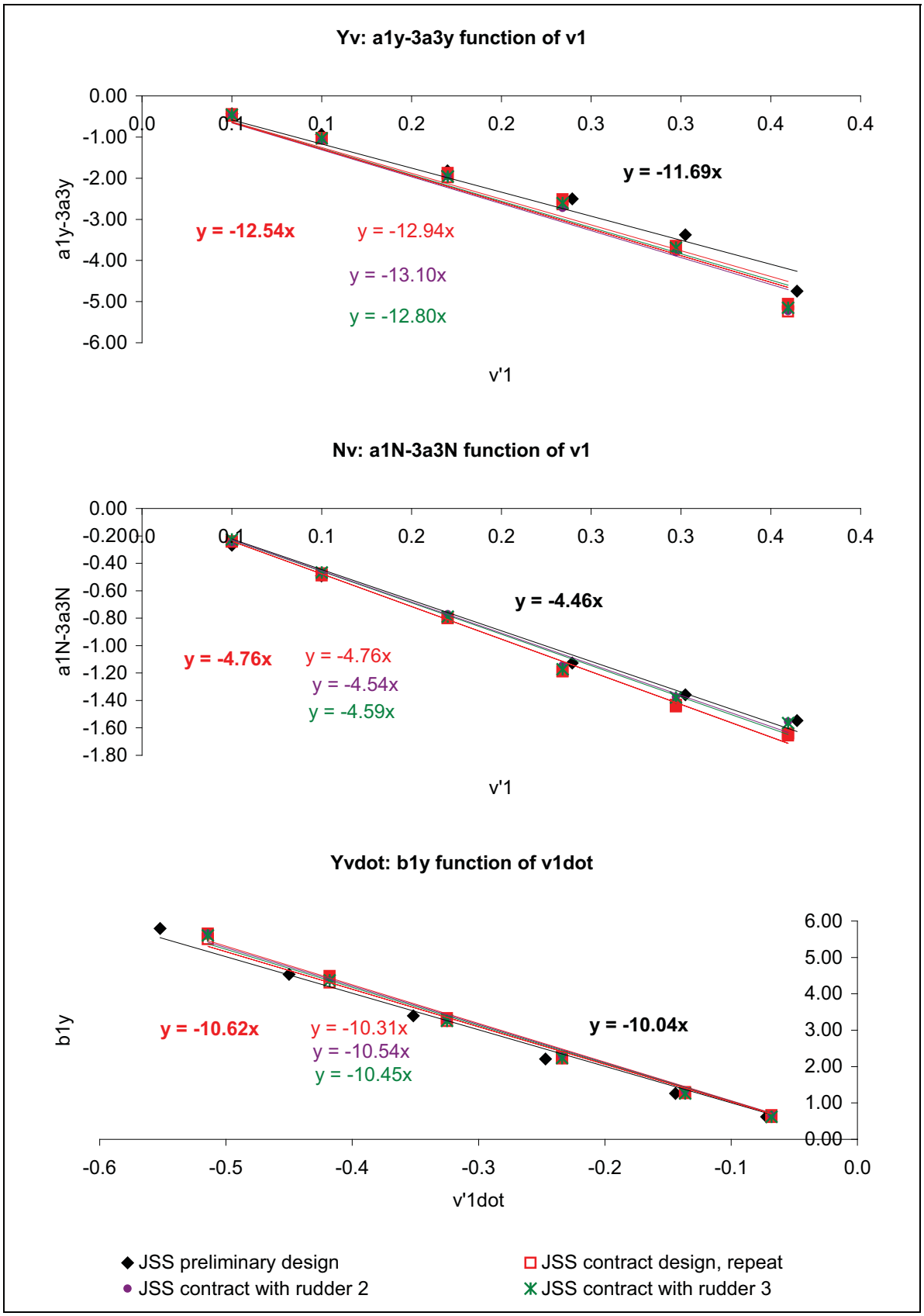

Figure 20. Multiple-Run Analysis: Linear Fit to Data from All Harmonic Sway Runs

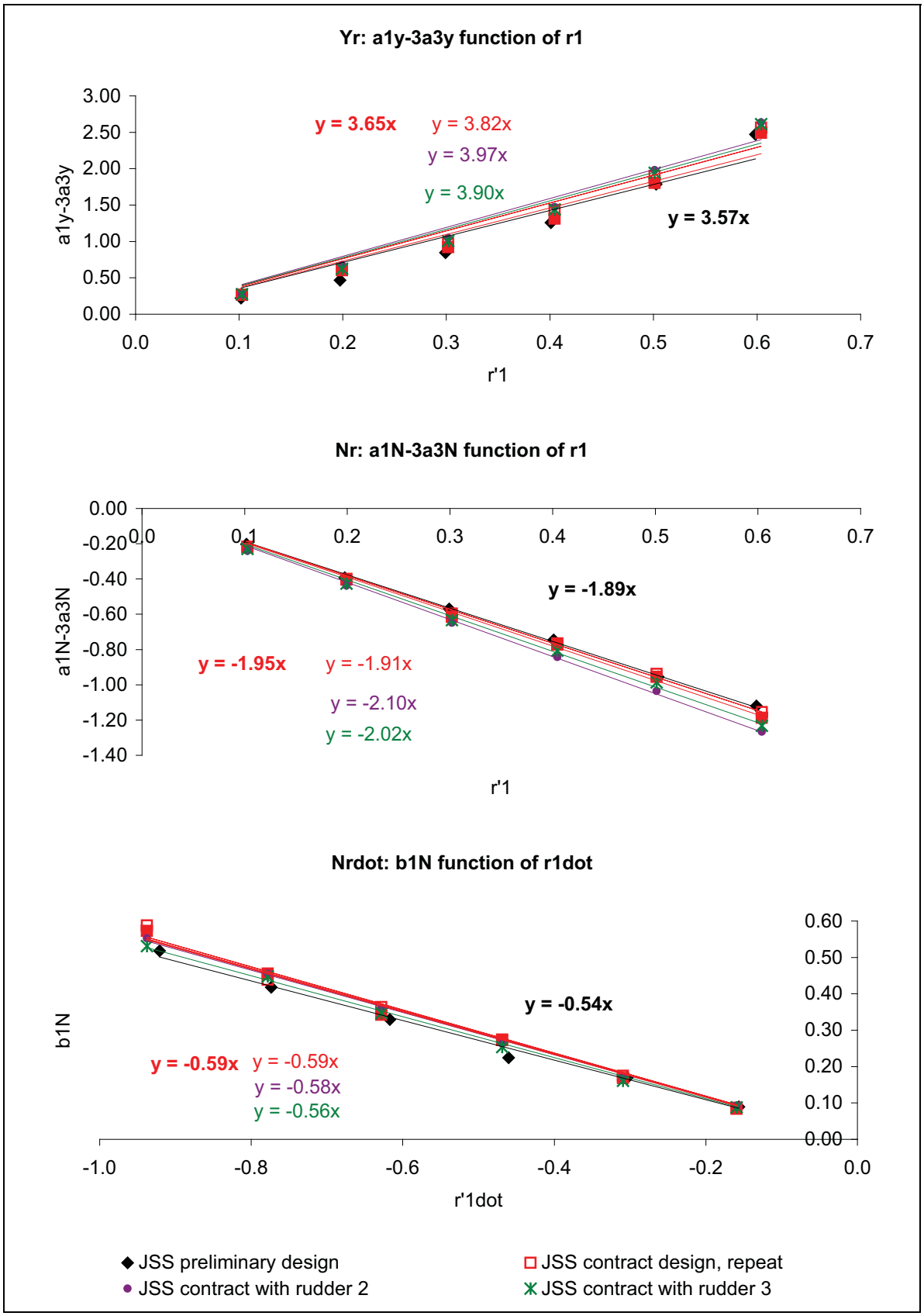

Figure 21. Multiple-Run Analysis: Linear Fit to Data from All Harmonic Yaw Runs

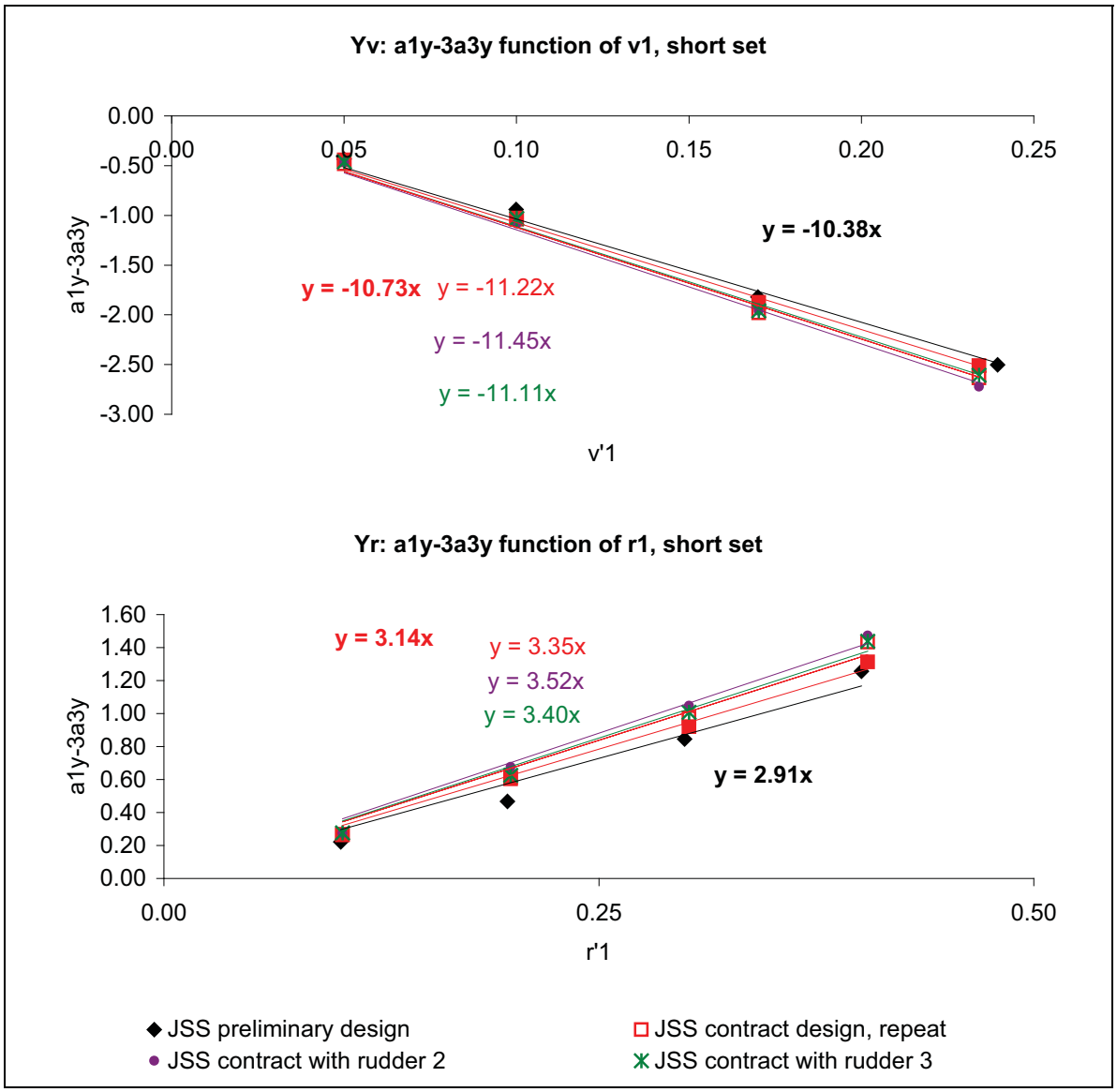

Figure 22. Multiple-Run Analysis: Linear Fit to Data from the four Lower Amplitude Motions

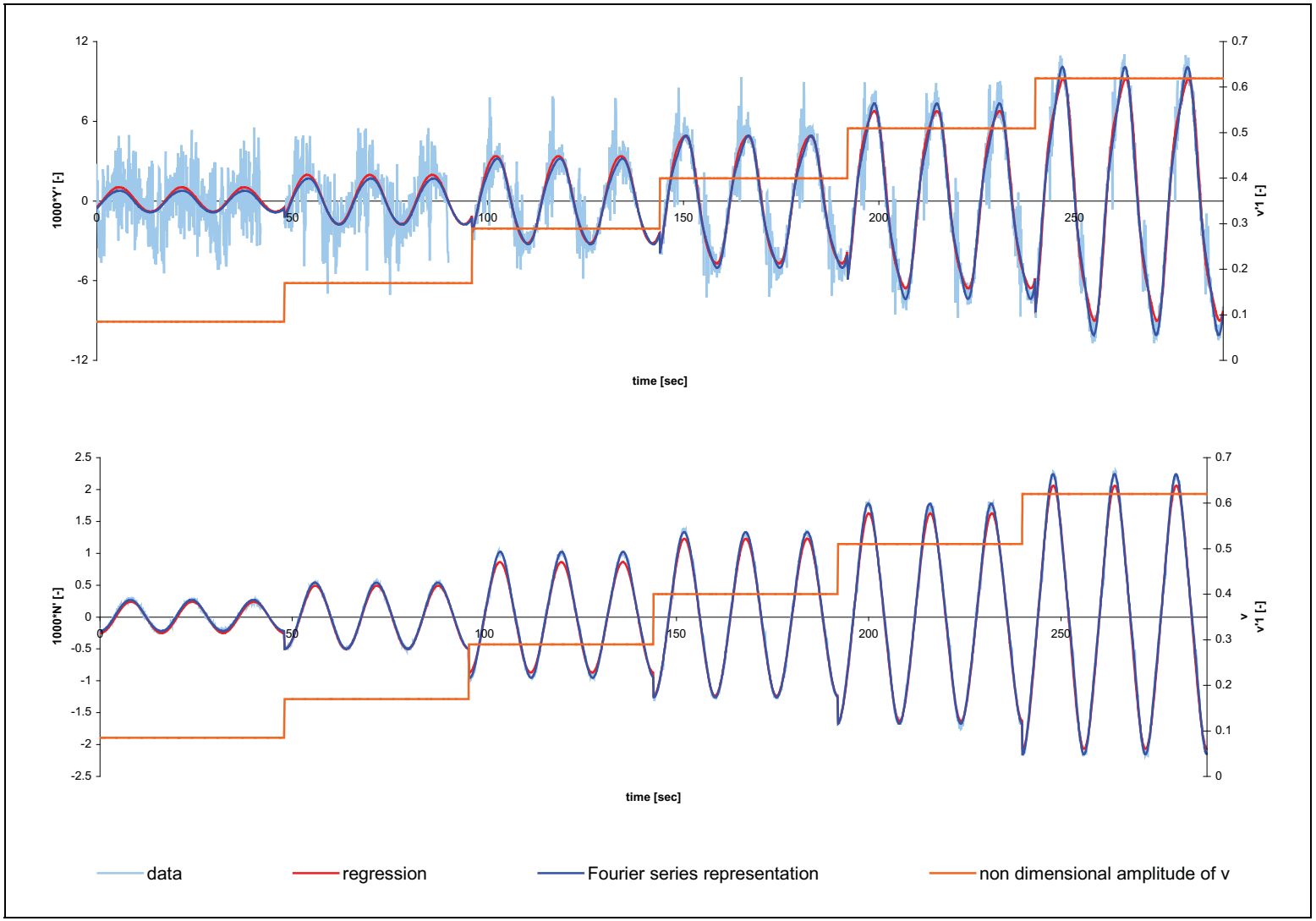

Figure 23. Direct Regression Analysis for JSS Contract Design: Pure Harmonic Sway Data and Regression Fit (Using Coefficients From Drift Tests)

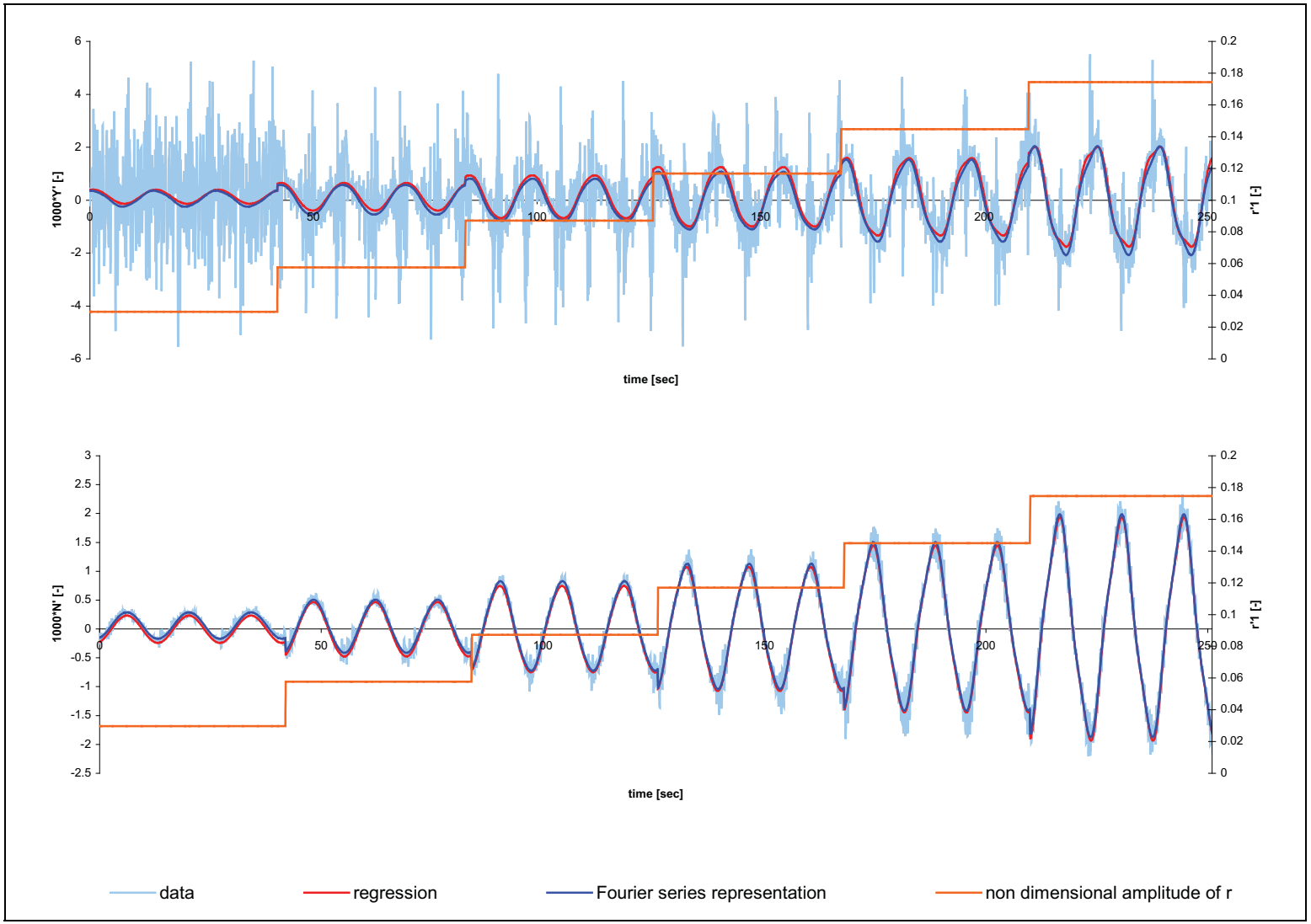

Figure 24. Direct Regression Analysis for JSS Contract Design: Pure Harmonic Yaw Data and Regression Fit

TABLES

		Design Rudder	Rudder 2	Rudder 3
Shaft CL Fwd of Transom	[m]	5.5	5.5	5.5
Tip Chord	[m]	4	7	5.516
Root Chord Along Hull	[m]	6.11	7	6.02
Span at shaft CL	[m]	7.018	7.018	7.018
Leading Edge Slope	[deg]	4.4	0	4.4
Section Profile		NACA0015	NACA0018	NACA0018

Table 1. Full Scale Dimensions of Rudders

HYDROSTATICS WITHOUT APPENDAGES	Scale 1:	29.77901
	Ship	Model
LENGTH BETWEEN PERPENDICULARS, m	174.85	5.871
LENGTH ON THE WATERLINE, m	180.34	6.056
LENGTH OVERALL, m	189.00	6.347
LENGTH OVERALL SUBMERGED, m	188.00	6.313
MAXIMUM WATERLINE BEAM, m	24.00	0.806
DRAFT AT MIDSHIPS, m	8.200	0.275
DRAFT ABOVE DATUM AT AFT PERPENDICULAR, m	8.200	0.275
DRAFT ABOVE DATUM AT FWD PERPENDICULAR, m	8.200	0.275
TRIM, deg.	0.000	0.000
EQUIVALENT LEVEL KEEL DRAFT ABOVE BASELINE, m	8.200	0.275
PARALLEL MIDDLE BODY WRT AP, m	NA	NA
TO, m	NA	NA
CENTRE OF BUOYANCY WRT AP, m	86.99	2.921
CENTRE OF BUOYANCY ABOVE BASELINE, m	4.46	0.150
CENTRE OF FLOTATION WRT AP, m	79.85	2.681
WATERPLANE AREA, sq. m	3739.27	4.217
WETTED SURFACE AREA, sq.m	5672.90	6.397
WETTED SURFACE AREA, (EXCLUDING TRANSOM) sq.m	5668.84	6.393
MIDSHIP SECTIONAL AREA, sq.m	194.50	0.219
TRANSVERSE METACENTRIC RADIUS, m	6.53	0.219
LONGITUDINAL METACENTRIC RADIUS, m	336.98	11.316
VOLUME OF DISPLACEMENT, cu. m	23924.22	0.906
DISPLACEMENT, (tonnes @ FS in SW)(kg @ MS in FW)	24522.33	904.50
MASS PROPERTIES		
CENTER OF GRAVITY ABOVE BASELINE, m	9.64	0.324
TRANSVERSE METACENTRE HEIGHT, m	1.34	0.045
LONGITUDINAL METACENTRE HEIGHT, m	331.79	11.142
APPENDAGES		
Bilge Keels		
CENTRE OF BUOYANCY WRT AP, m	87.50	2.897
VOLUME OF DISPLACEMENT, cu. m	4.52	0.0002
WETTED SURFACE AREA, sq.m	111.84	0.127
Rudder		
CENTRE OF BUOYANCY WRT AP, m	-0.92	-0.082
VOLUME OF DISPLACEMENT, cu. m	19.21	0.0007
WETTED SURFACE AREA, sq.m	79.42	0.090
Appended Displacement - Self Propulsion / PMM Experiments		
VOLUME OF DISPLACEMENT, cu. m	23947.96	0.9069
DISPLACEMENT, (tonnes @ FS in SW)(kg @ MS in FW)	24546.65	905.41
Appended Displacement - Resistance/Wake Survey Experiments		
VOLUME OF DISPLACEMENT, cu. m	23928.74	0.9061
DISPLACEMENT, (tonnes @ FS in SW)(kg @ MS in FW)	24526.96	904.67

Table 2. Model 911 Hydrostatics

COEFFICIENTS BASED ON:	LENGTH WATERLINE MAXIMUM BEAM AT WATERLINE EQUIVALENT LEVEL KEEL DRAFT
L/B	7.514
L/T	21.993
B/T	2.927
LCB %LBP FORWARD OF AP	49.749
LCF %LBP FORWARD OF AP	45.667
BLOCK COEFFICIENT	0.674
MIDSHIP COEFFICIENT	0.988
PRISMATIC COEFFICIENT	0.682
WATERPLANE COEFFICIENT	0.864
CIX Transverse Inertia of waterplane	0.752
CIY Longitudinal Inertia of waterplane	0.687
BM/B	0.272
BML/L	1.869
BEAM - DISPLACEMENT RATIO (CIRCB)	0.833
DRAFT - DISPLACEMENT RATIO (CIRCT)	0.285
LENGTH - DISPLACEMENT RATIO (CIRCM)	6.261
WETTED SURFACE - DISPLACEMENT RATIO (CIRCS)	6.830
BM - DISPLACEMENT RATIO	0.227
BML - DISPLACEMENT RATIO	11.699

Table 3. Model 911 Hydrostatic Coefficients

Mass properties relative to ship/model origin O, in model coordinates
O: design waterline, Station 5 (midship), centreline

	from bifilar experiment			from inclining experiment
oscillating mass of:	mass [kg]	xG fwd of O [m]	Izz about O [kg.m^2]	zG below O [m]
JSS contract design	794.7	-0.034	1752.3	0.0204
JSS contract design with Rudder 3	795.4	-0.037	1759.3	0.0204
JSS contract design with Rudder 2	796.1	-0.039	1765.4	0.0204

Table 4. Mass properties of the model oscillating mass

Project Name: JSS PMM Tests Project Number: 42_2517_16 Date: June 2012

Test	DAS	Name	Description	Units	Range	Resolution	Sample Rate (Hz)	Critical Level	Device	Excitation volts	Filter Hz
R,SP,PMM	OB	Thrust	Shaft Dynamometer Thrust	N	0-150	0.005	50	1	K&R R250		10
R,SP,PMM	OB	Torque	Shaft Dynamometer Torque	Nm	+/-6	0.001	50	1	K&R R250	+/- 15	10
R,SP,PMM	OB	Shaft Speed	Shaft Speed	rps	0-20	0.001	50	1			10
R,SP,PMM	TT	Inline Load	Inline Load	N	0-450	0.005	50	1	100 lb waterproofed S-Type	10	10
R,SP,PMM,WKS	TT	Tachogenerator	Carriage Speed using HR encoder	m/s	-0.5 - 2.5	0.0001	50	1			10
R,SP,PMM,WKS	TT	Carriage Speed	Carriage Position using Control system	m/s	-0.5 - 2.5	0.0001	50	1			10
PMM	OB	Rudder Angle	Rudder Angle	deg	+/- 40	0.005		1			10
PMM	OB	PMM Pitch	PMM Pitch	deg	+/-5		50	2			10
PMM	OB	PMM Yaw	PMM Yaw	deg	+/- 90		50	3	PT101-0030-111-1130		10
PMM	TT	Sway Displacement	PMM Sway	m	0-9		50	3	yoyo pot - PMM - 500"	10	10
PMM	OB	X1	PMM X1	mV	+/-10		50	1	R164-101-500N	5	10
PMM	OB	Y1	PMM Y1	mV	+/-10		50	1	R164-104-1920N	5	10
PMM	OB	Y2	PMM Y2	mV	+/-10		50	1	R164-105-1920N	5	10
PMM	OB	Z1	PMM Z1	mV	+/-10		50	1	R164-102-1920N	5	10
PMM	OB	Z2	PMM Z2	mV	+/-10		50	1	R164-103-1920N	5	10
PMM	OB	Z3	PMM Z3	mV	+/-10		50	1	R164-101-1920N	5	10
PMM	OB	Sinkage	Sinkage at PMM Tow Post	mm	0-650		50	2	30 inches yoyo pot	10	10
PMM	OB	PMM Start	PMM Start of Motions Step signal (OB)	V	+/- 10		500	1	PMM control panel	10	100
PMM	TT	DAS Trigger	PMM Start of Motions Step signal (Neff)	V	+/- 10		500	1	PMM control panel	10	100
PMM	TT	Yaw Velocity	PMM Yaw Velocity	deg/s	+/- 30		50	1	PMM control panel	10	10
PMM	TT	Sway Velocity	PMM sway Velocity	m/s	+/- 1.2		50	1	PMM control panel	10	10

OB On Board DAS (daspc49)
TT Carriage DAS (NEFF)

Table 5. List of Signals Measured and DAS Plan

Test	Speed [kts]	drift angle [deg]	Rudder angle d [deg]	Sway vel v' [-]	Yaw vel r' [-]	Propeller Shaft Speed
drift (+ rudder)	18	+/- 4, 8, 12, 16, 20	(-10), 0, (10)			ship self-propulsion
pure sway	18	N/A	0	0.05, 0.10, 0.17, 0.23, 0.30, 0.36	N/A	ship self-propulsion
pure yaw	18	0	0	N/A	0.10, 0.20, 0.30, 0.40, 0.50, 0.60	ship self-propulsion

Table 6. Test Matrix

Model surge u mean [m/s]	Model sway velocity v mean [m/s]	v' mean [-]	Yaw rate r mean [deg/s]	r' mean [-]	Drift Angle [deg]
1.6929	-0.1184	-0.07	na	na	4
1.6805	-0.2362	-0.14	na	na	8
1.6599	-0.3528	-0.21	na	na	12
1.6313	-0.4678	-0.28	na	na	16
1.5947	-0.5804	-0.34	na	na	20
1.6313	0.4678	0.28	na	na	-16
1.6599	0.3528	0.21	na	na	-12
1.6805	0.2362	0.14	na	na	-8
1.6929	0.1184	0.07	na	na	-4
1.5947	0.5804	0.34	na	na	-20

Table 7. Log of Drive Signals, Part 1: Drift Runs

scale =	29.77901	
Lpp=	5.8715	m
Uref =	1.697	m/s

	PMM file #	Cycles				Model surge u	Sway velocity v	Yaw rate r	non-dimensional amplitudes				equivalent max drift angle [deg]	smallest distance to tank wall
		T [sec]	number of cycles	ω'_1 [-]	length of one cycle along tank [Lpp]	mean [m/s]	v amplitude [m/s]	r amplitude [deg/s]	v amplitude	vdot amplitude	r amplitude	rdot amplitude		
harmonic sway	**39**	16	4.5	1.36	4.6	1.696	0.085		0.05	0.07			2.9	>3m
harmonic sway	**14**	16	4	1.36	4.6	1.693	0.17		0.10	0.14			5.7	>3m
harmonic sway	**15**	16	4	1.36	4.6	1.685	0.29		0.17	0.23			9.7	>3m
harmonic sway	**16**	16	4	1.36	4.6	1.673	0.4		0.24	0.32			13.3	>3m
harmonic sway	**17**	16	4	1.36	4.6	1.659	0.51		0.30	0.41			16.7	>3m
harmonic sway	**18**	16	4	1.36	4.6	1.640	0.62		0.37	0.50			20.1	>3m
harmonic sway	**19**	20	3	1.09	5.8	1.659	0.51		0.30	0.33			16.7	2.963 m
harmonic yaw	**21**	14	4.5	1.55	4.0	1.697		1.7			0.10	0.16		>3m
harmonic yaw	**22**	14	4.5	1.55	4.0	1.697		3.3			0.20	0.31		>3m
harmonic yaw	**23**	14	4.5	1.55	4.0	1.697		5.0			0.30	0.47		>3m
harmonic yaw	**24**	14	4.5	1.55	4.0	1.697		6.7			0.40	0.63		>3m
harmonic yaw	**25**	14	4.5	1.55	4.0	1.697		8.3			0.50	0.78		>3m
harmonic yaw	**26**	14	4.5	1.55	4.0	1.697		10.0			0.60	0.94		2.700 m
harmonic yaw	**27**	17	3.5	1.28	4.9	1.697		6.7			0.40	0.52		2.851 m

Table 8. Log of Drive Signals, Part 2: Harmonic Runs

Rho (ship)	1025.00	kg/m^3
kzz (Ship)	40.2155	m

	contract design	(preliminary design)	
Disp (Ship)	24522	23725	tonnes (SW)
xG (LCG)	0.508		m fwd of O
Lpp (Ship)	174.846	173.00	m
LWL	180.0	180.0	m
Lpp/T	21.32	21.68	
Scale	29.77901	29.68905	

Ship non-dimensional mass and inertia:

m' *1000	8.95	8.94
I'z *1000	0.474	0.483
x'G	0.0029	

m' = m/(0.5*Rho*Lpp^3)
I'z = (m*kzz^2)/(0.5*Rho*Lpp^5)
x'G=xG/Lpp

Table 9. Mass and Moment of Inertia for JSS Contract Design Ship

*1000	JSS Contract	JSS contract repeat	with Rudder 3	with Rudder 2
Y'v	-11.32	-11.73	-11.46	-12.18
N'v	-4.89	-4.99	-4.92	-4.92

Table 10. Non-Dimensional Hydrodynamic Coefficients from Drift Tests

Linear fit over all harmonic runs

Configuration	JSS contract design	JSS contract design, repeat	JSS contract design, with Rudder 3	JSS contract design, with Rudder 2	Preliminary design
Rudder Skeg shaft speed	design rudder none ship self-propulsion	design rudder none ship self-propulsion	Rudder 3 none ship self-propulsion	Rudder 2 none ship self-propulsion	design rudder none ship self-propulsion
Y'v *1000	-12.54	-12.94	-12.80	-13.10	-11.69
N'r *1000	-1.95	-1.91	-2.02	-2.10	-1.89
Y'r *1000	3.65	3.82	3.90	3.97	3.57
N'v *1000	-4.76	-4.76	-4.59	-4.54	-4.46
Y'vdot *1000	-10.62	-10.31	-10.45	-10.54	-10.04
N'rdot *1000	-0.59	-0.59	-0.56	-0.58	-0.54
A' *10^6	20.74	20.54	20.09	20.55	19.33
B' *10^6	51.48	50.62	52.52	54.71	47.73
C' *10^6	-0.7	0.3	2.7	4.9	-2.0
sigma1	0.01	-0.01	-0.05	-0.09	0.04

Information from earlier tests

A' is (I'z-N'rdot)*(m'-Y'vdot)
B' is -(I'z-N'rdot)*Y'v-(m'-Y'vdot)*N'r
C' is Y'v*N'r-N'v*(Y'r-m')

Non-dimensionalization uses the following quantities:
distance: Lpp
speed: instantaneous speed along track

Linear fit over the four lower amplitude runs for determination of Yv and Yr, and all runs for other coefficients

Configuration	JSS contract design	JSS contract design, repeat	JSS contract design, with Rudder 3	JSS contract design, with Rudder 2	Preliminary design
Rudder Skeg shaft speed	design rudder none ship self-propulsion	design rudder none ship self-propulsion	Rudder 3 none ship self-propulsion	Rudder 2 none ship self-propulsion	design rudder none ship self-propulsion
Y'v *1000	-10.73	-11.22	-11.11	-11.45	-10.38
N'r *1000	-1.95	-1.91	-2.02	-2.10	-1.89
Y'r *1000	3.14	3.35	3.40	3.52	2.91
N'v *1000	-4.76	-4.76	-4.59	-4.54	-4.46
Y'vdot *1000	-10.62	-10.31	-10.45	-10.54	-10.04
N'rdot *1000	-0.59	-0.59	-0.56	-0.58	-0.54
A' *10^6	20.74	20.54	20.09	20.55	19.33
B' *10^6	49.56	48.79	50.77	52.97	46.39
C' *10^6	-6.7	-5.2	-3.0	-0.6	-7.4
sigma1	0.13	0.10	0.06	0.01	0.15

Information from earlier tests

Table 11. Hydrodynamic Coefficients and Stability Assessment of JSS Contract Design, Using "Multiple-Run" Analysis of Harmonic Runs

Configuration	with v coefficients determined from drift tests: JSS contract design	JSS contract design, repeat	JSS contract design, with Rudder 3	JSS contract design, with Rudder 2	with v coefficients determined from the harmonic sway tests: JSS preliminary design	JSS contract design
Rudder	design rudder	design rudder	Rudder 3	Rudder 2	design rudder	design rudder
Skeg	none	none	none	none	none	none
shaft speed	ship self-propulsion	ship self-propulsion	ship self-propulsion	ship self-propulsion	ship self-propulsion	ship self-propulsion
Y'v *1000	-11.32	-11.73	-11.46	-12.18	-8.95	-11.33
N'r *1000	-2.11	-2.08	-2.18	-2.23	-1.90	-2.11
Y'r *1000	2.42	2.60	2.66	2.81	2.33	2.42
N'v *1000	-4.89	-4.99	-4.92	-4.92	-4.66	-4.96
Y'vdot *1000	-10.58	-10.27	-10.40	-10.49	-9.14	-10.58
N'rdot *1000	-0.56	-0.58	-0.54	-0.49	-0.49	-0.57
A' *10^6	20.23	20.21	19.57	18.78	17.55	20.37
B' *10^6	52.98	52.38	53.68	55.20	43.12	53.07
C' *10^6	-8.1	-7.3	-6.0	-3.0	-13.7	-8.5
sigma1	0.14	0.13	0.11	0.05	0.29	0.15

from earlier tests

A' is (I'z-N'rdot)*(m'-Y'vdot)
B' is -(I'z-N'rdot)*Y'v-(m'-Y'vdot)*N'v
C' is Y'v*N'r-N'v*(Y'r-m')

Non-dimensionalization uses the following quantities:
distance: Lpp
speed: instantaneous speed along track

Table 12. Hydrodynamic Coefficients and Stability Assessment of JSS Contract Design, Using Direct Regression Analysis